

SEISMIC REFRACTION ANALYSIS OF EAST RIVER FLATS MINNEAPOLIS
MINNESOTA

A THESIS
SUBMITTED TO THE FACULTY OF
UNIVERSITY OF MINNESOTA
BY
AUTUMN HAAGSMA

IN PARTIAL FULFILLMENT OF THE REQUIREMENTS
FOR THE DEGREE OF
MASTER OF SCIENCE

Justin Revenaugh

October 2013

Seismic Refraction Analysis of East River Flats Minneapolis Minnesota ©Oct 2013

Acknowledgements

I would like to thank my advisor Justin Revenaugh for guiding and supporting me throughout my thesis. I would also like to thank my husband, Ricky Haagsma, for ripping his shorts to provide me with good data.

Dedications

I dedicate this thesis to my always supportive husband and to my son.

Abstract

East River Flats, a city park along the Mississippi River, was analyzed using Geometrics SmartSeis seismograph and 16 geophones. Refraction calculations and models were done using 1D and 2D time-term inversion methods. The results yielded a 3 layer model which consisted of a low velocity top soil, water saturated sand and gravel, and highly fractured Platteville formation limestone.

Table of Contents	
List of Tables	V
List of Figures	VI
Introduction	1
Methods	3
Data and Results	13
Conclusions	22
Bibliography	24
Appendix	25

List of Tables

Table 1: Equipment Specifications	4
Table 2: Compiled travel times for W-E Survey	14
Table 3: Compiled travel times for N-S Survey	15
Table 4: Calculated velocities and depths for W-E Survey	15
Table 5: Calculated velocities and depths for N-S Survey	16
Table 6: Reciprocity errors for W-E Survey	18
Table 7: Reciprocity errors for N-S Survey	18
Table 8: Measured velocities of different materials (Kohnen 1974)	21

List of Figures

Figure 1: Image of East River Flats	2
Figure 2: Stratigraphic Column of Local Geology	3
Figure 3: Schematic of Survey Geometry	5
Figure 4: Images of Field equipment	5
Figure 5: Schematic of refracting waves	7
Figure 6: Examples of raw and filtered data	9
Figure 7: Travel time plot	10
Figure 8: Schematic of refracting waves	11
Figure 9: Compiled travel time plot W-E survey	16
Figure 10: Compiled travel time plot N-S survey	17
Figure 11: Model of W-E survey	19
Figure 12: Model of N-S survey	19
Figure 13: Travel times highlighting possible fracture	22

Introduction

The East River Flats is a city park at 44°58'12.89N and 93°24'5.64W, which is located south of Coffman Hall on the University of Minnesota Twin Cities campus (figure 1). The area is mostly flat and lies adjacent to the Mississippi River. The Mississippi River is about 5 meter below the edge. The surface consists of patches of grass and unconsolidated sediments.

The unconsolidated sediment contains soil and mostly gravel, sand, and silt of various rock types which were deposited by the Mississippi River. Underneath this layer lies the Platteville Formation which is highly fractured limestone that often contains fossils. Below this lies a thin layer of shale called the Glenwood Formation (often not seen) followed by St. Peter Sandstone which consists of loosely cemented quartz grains. These three Ordovician formations make up the Mississippi River Valley in the Twin Cities area (Figure 2). (Madigan, 2003)



Figure 1: East river flats is located behind Coffman Hall on the University of Minnesota Twin Cities campus. The markers and red lines mark where the survey was taken. Image B is zoomed out to show geographic location relative to campus.

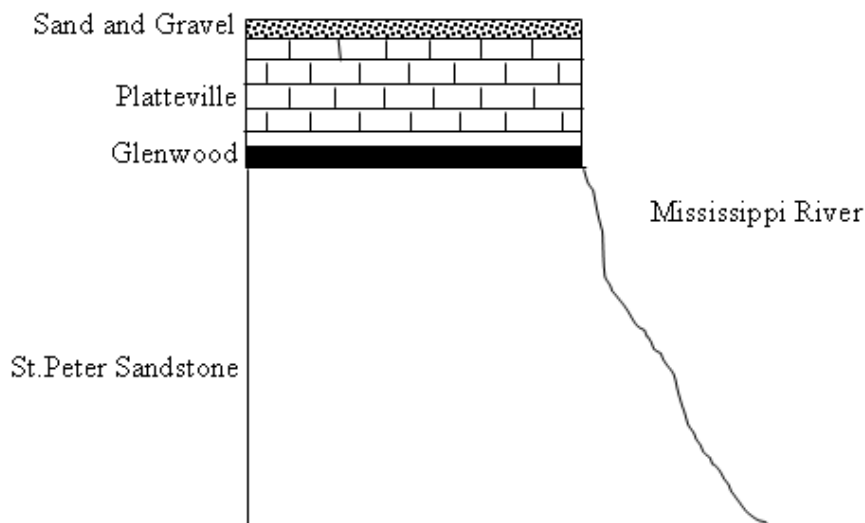


Figure 2: Overly simplified stratigraphic column of the geology along the Mississippi River at East River Flats (not to scale).

The unconsolidated sediments on the surface along the Mississippi River vary in thickness at different locations due to different depositional events and methods. The thickness of these deposits could also change perpendicular to the river. A seismic refraction survey of the East River Flats area will reveal the thickness in this area and if that thickness changes with proximity to the Mississippi River. The survey can also be used to determine the height of the water table and to calculate the porosity of the overlying sediments.

Methods

On July 30 2013 travel time data was collected using a Geometrics SmartSeis exploration seismograph with 16 moving-coil geophones. July 30th was a clear sunny day with little to no wind. The ground was dry but it rained lightly the night before making the surface less hard than usual. The first survey was set up roughly running west to east to run parallel to the Mississippi river. The SmartSeis seismograph was set up using the

recommended settings (table 1). The geophones were placed 4 meters apart for a total offset of 60 meters. The energy source was a 20lb sledge hammer and a metal strike plate. The first shot was 8 meters off of geophone 1 with a shot spacing of 8 meters (every other geophone). See figure 3 and 4 below for an example of the survey geometry and pictures of the equipment. 20 strikes of the hammer at each shot location were stacked to enhance results. No filters were applied in the field and when a shot occurred next to a geophone that geophone was turned off so as not to skew the data.

Recorder	Geometrics SmartSeis ST Seismograph
number of channels	12
sample rate	500 μ s
record length	1024 ms
field filters	out
delay time	10 ms
Source	20lb sledge hammer and strike plate
stacks per record	20
Geophones	16 Geospace GS-20DX/PC-801LPC
natural frequency	14 Hz
bandwidth	1.75Hz-8000Hz
Power	12-volt battery

Table 1: Equipment specifications

A second survey was set up to cross the middle of the first, running perpendicular to the river, running north to south (see figure 1). Only 9 geophones were used instead of the 16 because of the available space and proximity to sidewalks. The geophones were spaced 4 meters apart and the shots were spaced 8 meters apart starting at 4 meters off of geophone 1. The same source was used and swung 20 times, with vertical stacking at each shot.

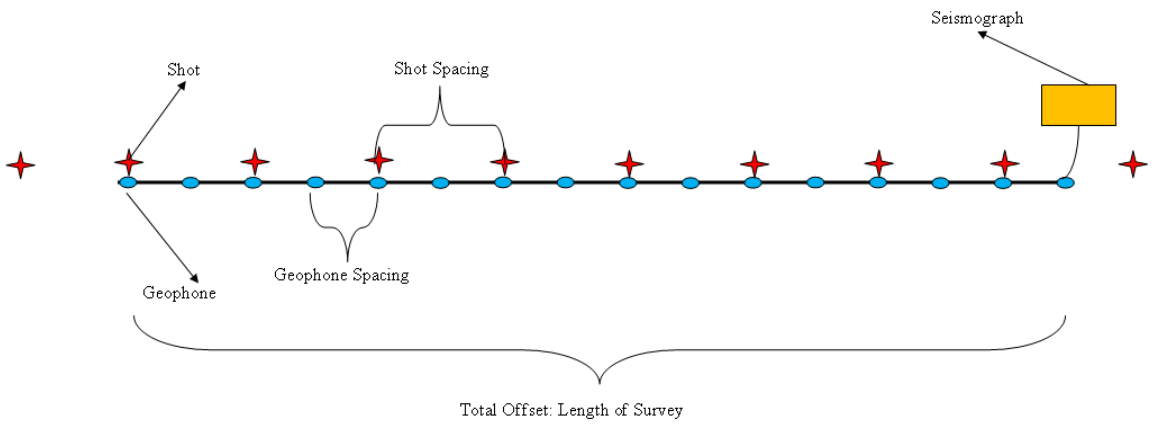


Figure 3: A schematic drawing of the survey geometry. Each blue dot represents a geophone and each red star represents a shot location.



Figure 4: Pictures taken in the field during the survey. Image A shows the survey line. A blue geophone is located at each orange flag. Image B shows the SmartSeis Seismograph located at the end of the survey.

The time it takes for the seismic wave to reach each geophone (travel time) along with the geophone location is recorded. There are several methods that can be used to evaluate this data. Due to the simplicity of the geology, there is no need to use complex methods. Two methods were chosen; a 1D analysis which assumes flat, horizontal layers

with no lateral depth variations in the layers, and a 2D time-term inversion method which allows for lateral variations in depth. Both methods assume a constant velocity through each layer.

1D Model

Seismic waves travel through the earth at differing velocities interacting with boundaries and responding to changes in bulk and shear modulus and density. Refracted waves can interact three ways with layer boundaries: when a wave hits the boundary it can reflect, possibly with a change in mode (P to S or vice versa), travel along the boundary as a “headwave” before returning to the surface, or penetrate the boundary, again with the possibility of a mode change, and continue at a different angle than before. All of these options are available and the geometry of the interactions is dictated by Snell’s law (1). Figure 5 below demonstrates one of the possible paths of the refracted wave.

$$\frac{\sin(i)}{v_1} = \frac{\sin(i_c)}{v_2} = \frac{1}{v_2} \quad (1)$$

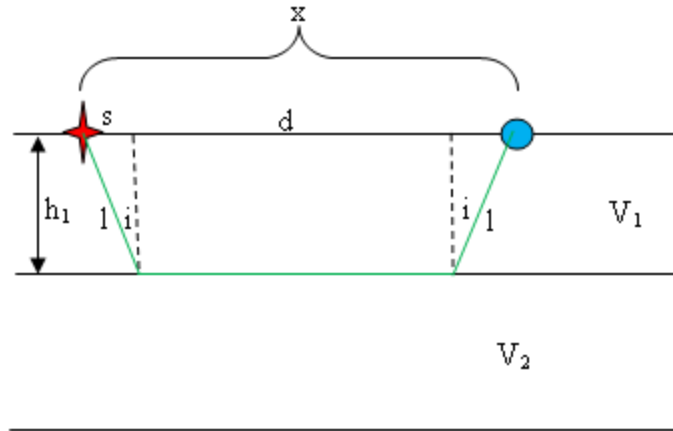


Figure 5: Schematic drawing of a refracted wave (green) traveling from energy source (red star) through layer 1 and along the boundary at velocity 2 before traveling up to the geophone (blue dot).

The time it takes for the direct wave (t_0), which travels directly from the source (s) to the geophone (blue dot), is simply the distance divided by the velocity (2). The time it takes for the first refracted wave (T_H), or head wave, to reach a geophone can be derived by following the refracted wave path, green line in figure 3.

$$t_0 = \frac{x}{v_1} \quad (2)$$

$$T_H = \frac{2l}{v_1} + \frac{d}{v_2} \quad (3)$$

Equation 3 can be combined with Snell's Law (1) to put it in terms of length, depth, and velocity. The derivative of equation 2 and equation 3 yields the velocities of the first and second layers (5 and 6).

$$T_H = \frac{x}{v_2} + \frac{2h_1}{v_1} \frac{\sqrt{v_2^2 - v_1^2}}{v_2} \quad (4)$$

$$\frac{dt_0}{dx} = \frac{1}{v_1} \quad (5)$$

$$\frac{dT_H}{dx} = \frac{1}{v_2} \quad (6)$$

Similar methods can be applied to derive an equation to find the velocity of a third layer if one is present. The ray path would travel down through layer 1, change angles at layer 2/layer1 boundary due to density differences, and then travel along layer 3 boundary before traveling back up following a symmetric path.

$$T_3 = \frac{x}{v_3} + \frac{h_1 \sqrt{v_3^2 - v_1^2}}{2v_3 v_1} + \frac{h_2 \sqrt{v_3^2 - v_2^2}}{v_3 v_2} \quad (7)$$

$$\frac{dT_3}{dx} = \frac{1}{v_3} \quad (8)$$

Then, after some algebra, equations 5 and 7 can be solved for the thicknesses of layer 1 and layer 2.

$$h_1 = \frac{TV_2 V_1}{2\sqrt{v_2^2 - v_1^2}} \quad (9)$$

$$h_2 = \frac{1}{2} \left(T - 2h_1 \frac{\sqrt{v_3^2 - v_1^2}}{v_3 v_1} \right) \frac{v_3 v_2}{\sqrt{v_3^2 - v_2^2}} \quad (10)$$

Pickwin, part of the SeisImager software package provided by Geometrics, was used to identify the first arrival times at each geophone. Background noise from nearby roads, power lines, trees, and construction projects sometimes made selecting the first arrivals difficult. High and low filters were applied to each data set until the first arrivals could be identified. Pickwin has a built in first pick tool, but it was not always reliable. If

a first pick was hard to identify after applying filters, then the first pick took was used to help with identification. If a first arrival was not visible or was not in line with the others, then it was omitted.

Figure 6 demonstrates the process of selecting first picks. In image (a), the unfiltered data, the first arrivals are hidden. After applying hi and low filters, the first arrivals can be identified in image (b). Lines were drawn to estimate velocity and verify the selection of the first arrivals. See appendix to view all first picks.

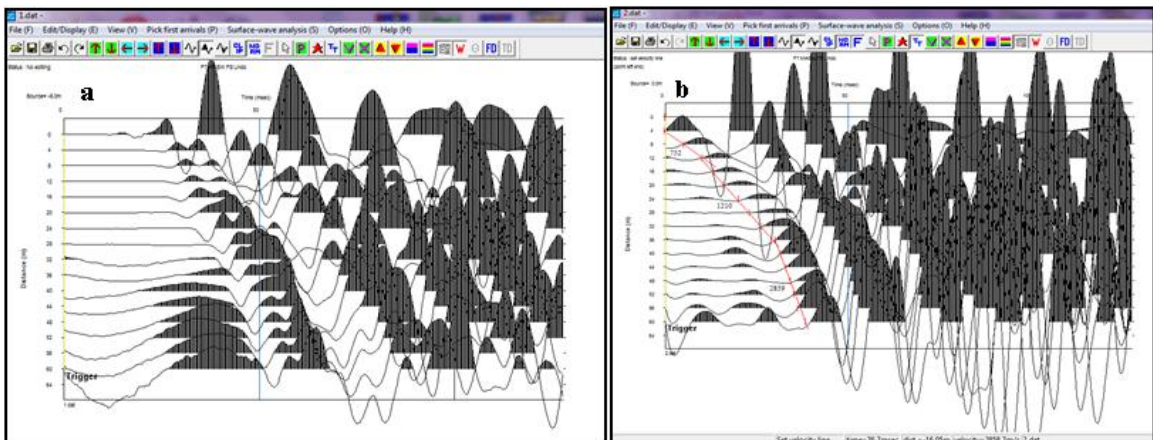


Figure 6: Image (a) is an example of unfiltered raw data. Image (b) is an example of filtered data with selected first picks (red vertical dashes) and velocity lines (red lines).

After the first arrivals were selected, they were plotted using Plotrefa (another program which is a part of the Geometrics SmartSeis software) and Microsoft excel to calculate the velocities using equations (5,6, and 8). The inverse of the plotted slopes are the velocities of each layer. Figure 7 is an example of the plotted data from figure 6. Once the velocities were calculated for each layer, the depths of the layers were calculated using equations (9 and 10).

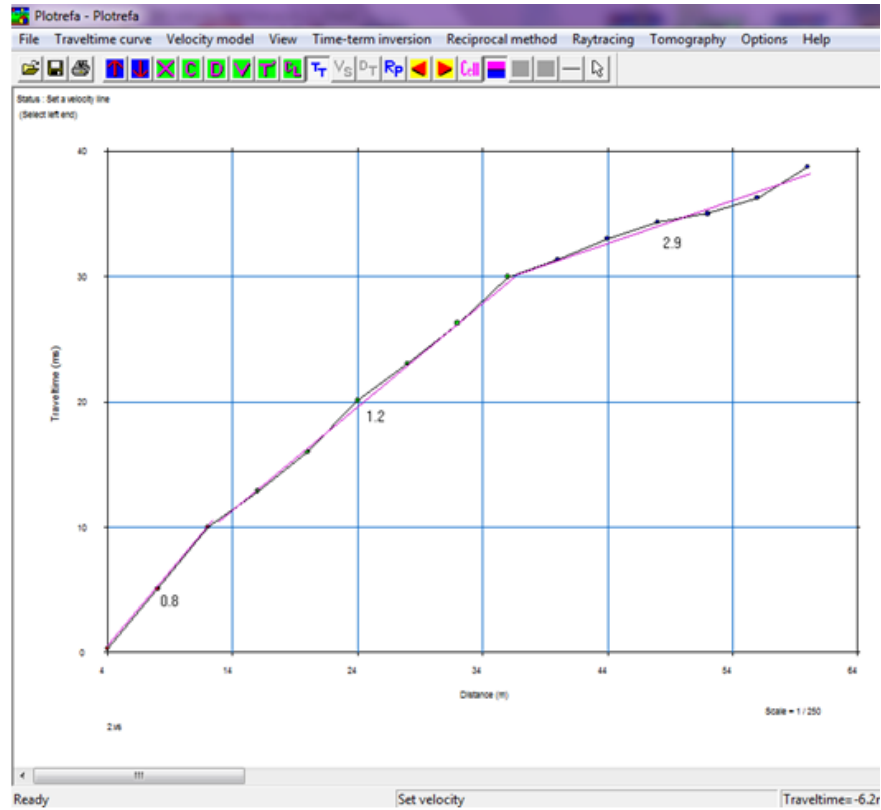


Figure 7: Travel-time plot with velocity lines (red) and calculated velocities (km/s) shown below each velocity line.

Time-Term Inversion

Time-term inversion follows a similar reasoning as the 1D model above, with one major difference: the ray-paths do not have to be symmetric which allows for lateral variations in depths. See figure 8 below.

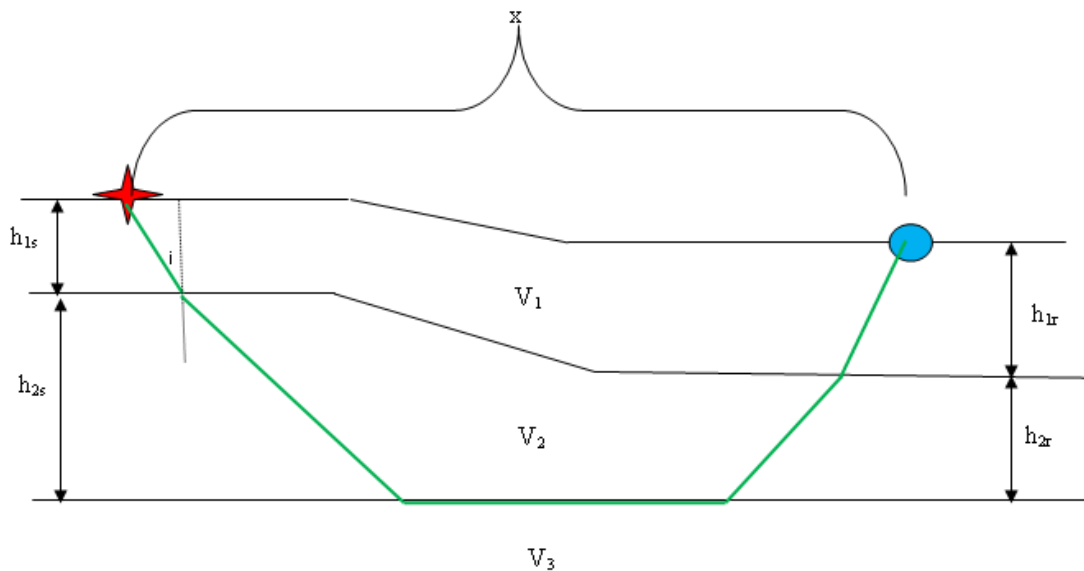


Figure 8: The green line above represents a refraction path through layers which have lateral variations. The red star represents the source (s) and the blue dot represents a geophone (r).

The derivation begins by following the ray-path (green line) through the layers. D_s and D_r are the time terms which accounts for different angles and depths. The subscript s denotes the source side and the subscript r denotes the geophone (receiver) side.

$$t = \frac{x}{V} + D_s + D_r \quad (11)$$

The travel times then become:

$$t = \frac{x}{V_n} + \sum_{i=1}^{n-1} \left(\frac{h_{is} \cos i_{is}}{V_i} \right) + \sum_{i=1}^{n-1} \left(\frac{h_{ir} \cos i_{ir}}{V_i} \right) \quad (12)$$

Where;

$$\cos i_i = \sqrt{1 - \left(\frac{V_i}{V_n} \right)^2} \quad (13)$$

The velocities are calculated the same way as in the 1D model. The derivative of the travel time equation yields:

$$\frac{dt}{dx} = \frac{1}{v_n} \quad (14)$$

Travel times are calculated for M shots and N stations producing MN travel time equations. There are many more equations than there are unknowns. This means there is not a singular solution to the system of equations. Instead, the least squares method is applied to reduce the system down to the best fit solution. The Geometrics PlotRefa program assumes that the travel times take on the form of:

$$\underline{t} = \underline{A} \underline{m} \quad (15)$$

where matrix A is $M \times N$ (#shots \times #stations). The vector m must be chosen so that it minimizes L_2 (equation 16).

$$\left\| \underline{A} \underline{m} - \underline{t} \right\|^2 = L_2 \quad (16)$$

Equation 16 was expanded and the derivative taken with respect to m to minimize it. This produced a solution for m :

$$\underline{m} = (\underline{A}^T \underline{A})^{-1} \underline{A}^T \underline{t} \quad (17)$$

The solution can further be reduced by next assuming the form:

$$\underline{G}(\underline{m}) = \underline{t} \quad (18)$$

where $\underline{m} = \underline{m}_0 + \underline{\delta m}$. An initial estimate of \underline{m}_0 is chosen so that it is close to the correct value. The value can be chosen from the 1D model calculations. Next, the equation is

solved using least squares again to calculate $\underline{m_1}$. The final result will contain velocities for each layer, and depths at each geophone.

Data and Results

The first arrivals for each shot were selected and compiled in tables 2 and 3. The first arrivals were chosen by first using the first pick tool. Pickwin marked where it interpreted the first arrival to be. This was useful when the first arrival was obvious, otherwise the pick was off. The first arrivals could be identified by the first noticeably different spike in the signal. High and low frequency filters were used to reduce the background noise and make the first arrivals more visible. Amplitude of the signals was increased or decreased to help better locate a pick as well. If a first arrival was not visible or did not line up with the others, it was ignored.

The first arrival times were plotted with the x-offset in Microsoft Excel. Figures 9 and 10 show compiled plots of all shots for the two survey lines. All of the first arrivals chosen in Pickwin and the excel plots can be found in the appendix. The velocities and depths were calculated using the 1D method and compiled into tables 3 and 4. If velocity lines from different shots crossed each other or came close, the data was reevaluated to see if a better selection of first arrivals could be made. Velocity lines of different shots should not cross. In the best case scenario they would be parallel.

The calculated depths for the W-E survey (see table 3) suggests that the second survey was not long enough to observe a third layer. The survey line was 32 meters in length. Generally, depth of the survey would be $\frac{1}{4}$ of the survey length. The maximum depth that could be observed would be 8 meters. The estimated depth to the third layer

based off the W-E survey was 10-12 meters. The velocities and depths for the N-S survey were calculated based on a two-layer scenario.

The velocities calculated in the N-S survey were higher than those calculated for the W-E survey. This could be due to less data and the influence of end points being part of layer three. The velocity anomaly could also be due to lateral variations in velocity. The N-S survey could be been located over an area of lower velocity. The change in velocity could be from a density change.

		W-E Survey First Arrivals (ms)									
Shot/Geophone Position (m)	shot 1	shot 2	shot 3	shot 4	shot 5	shot 6	shot 7	shot 8	shot 9	shot 10	
-8	0.00										
0	10.35	0.15	16.90	33.30	42.30	43.70	46.55	51.10	53.05	56.75	
4	22.00	8.10	5.60	28.50	38.25	41.75	44.25	49.23	51.85	54.65	
8	32.25	16.55	0.00	15.50	35.60	40.20	43.00	47.75	49.90	52.55	
12	35.50	26.45	6.15	7.75	26.25	36.50	41.95	46.55	48.10	51.10	
16	38.60	35.60	15.85	0.00	17.60	31.90	40.90	44.50	47.05	49.55	
20	41.05	38.05	25.35	5.75	7.55	26.95	38.00	43.86	45.25	48.10	
24	43.70	40.70	31.50	16.25	0.00	16.00	34.70	42.50	44.00	46.55	
28	45.65	42.85	34.70	29.00	7.20	7.55	26.25	41.60	42.25	45.85	
32	46.90	44.40	39.65	35.75	15.65	0.00	18.85	36.85	40.70	44.05	
36	48.45	45.50	41.60	37.20	26.25	8.45	8.25	33.85	39.50	42.30	
40	50.05	46.70	42.50	40.25	36.50	18.65	0.00	23.80	36.25	40.35	
44	51.45	48.45	44.75	41.25	38.75	27.50	7.20	8.80	33.50	37.00	
48	53.40	50.40	46.20	42.75	41.25	32.05	19.00	0.00	22.75	32.60	
52	54.80	51.25	47.75	44.75	42.65	36.30	28.70	7.90	10.75	28.35	
56	56.75	52.25	49.35	47.00	43.90	40.35	34.20	16.70	0.00	21.50	
60	57.80	55.00	51.10	48.25	45.50	41.95	38.40	25.20	8.45	13.00	

Table 2: Compiled first arrival times (ms) for each shot at each geophone location.

	N-S Survey First Arrivals (ms)					
shot/geophone position	shot 1	shot 2	shot 3	shot 4	shot 5	shot 6
-4	0					
0	11.5	10.55	31.2	39.5	41.95	47.05
4	22.35	0	20.8	34.35	41.05	45.5
8	31.5	10.55	10.35	29.6	39.15	43.9
12	34.9	20.6	0	20.1	37.5	42.3
16	36.3	31.7	9.85	9.3	32.05	40.55
20	37.55	37.35	18.5	0	20.1	37.2
24	38.75	38.4	29.4	7.9	10.55	33.85
28	40.35	40.7	35.4	18.5	0	23.6
32	41.95	41.75	39.15	32.95	10.9	11
36	0					

Table 3: Compiled first arrival times (ms) for the second survey which crosses perpendicular to the first.

	W-E Survey Velocity (m/s)				
shot	layer 1	layer 2	layer 3	h1(m)	h2(m)
1	365.30	1406.07	2534.85	4.000376	8.025742
2	432.53	1639.34	2747.25	5.80249	6.152176
3	470.03	867.68	2468.53	3.370548	5.433543
4	419.60	712.96	2217.79	2.774325	7.031149
5	439.74	1439.05	2857.14	5.648158	6.198582
6	439.71	918.23	2392.86	3.596311	7.015681
7	433.12	1057.53	2941.18	4.360034	7.103978
8	408.57	1032.20	2949.85	4.879071	5.899682
9	414.46	1333.33	2615.75	5.323725	4.859253
10	427.59	924.81	2457.00	3.701081	6.617591

Table 4: Velocity calculations for each layer at each shot using the inverse of the plotted slopes.

N-S Survey $V(m/s)$			
shot	layer 1	layer 2	$h_1(m)$
1	400.00	1606.94	5.06
2	379.77	1705.61	5.11
3	398.71	1066.67	4.58
4	383.53	1012.66	3.66
5	372.70	1713.21	5.09
6	350.12	1880.76	5.12

Table 5: Velocity calculations for each layer at each shot using the inverse of the plotted slopes.

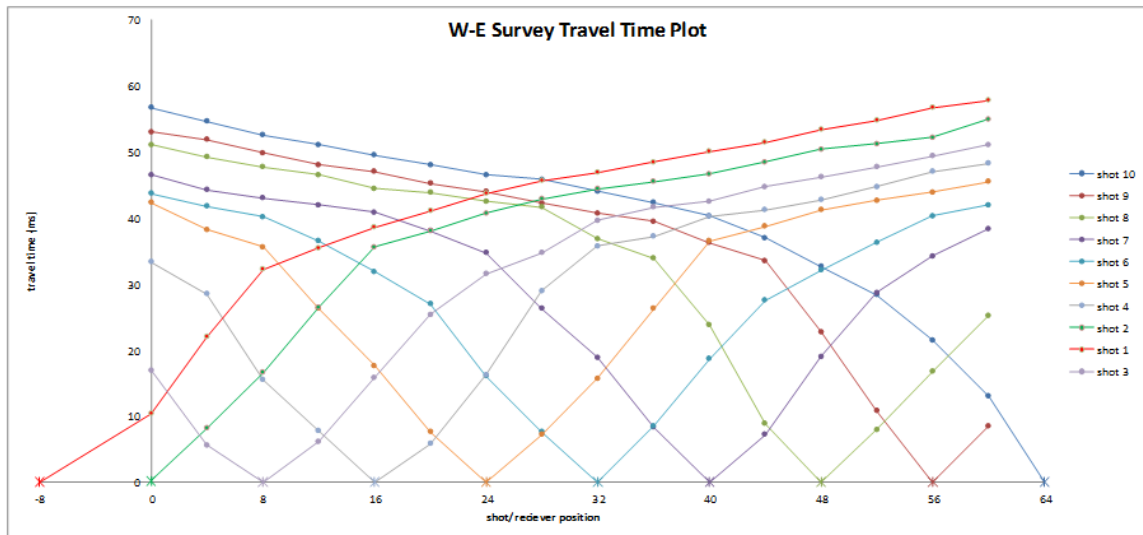


Figure 9: Compiled travel time plots of the W-E survey. Each star represents a shot location and each dot represents a geophone location.

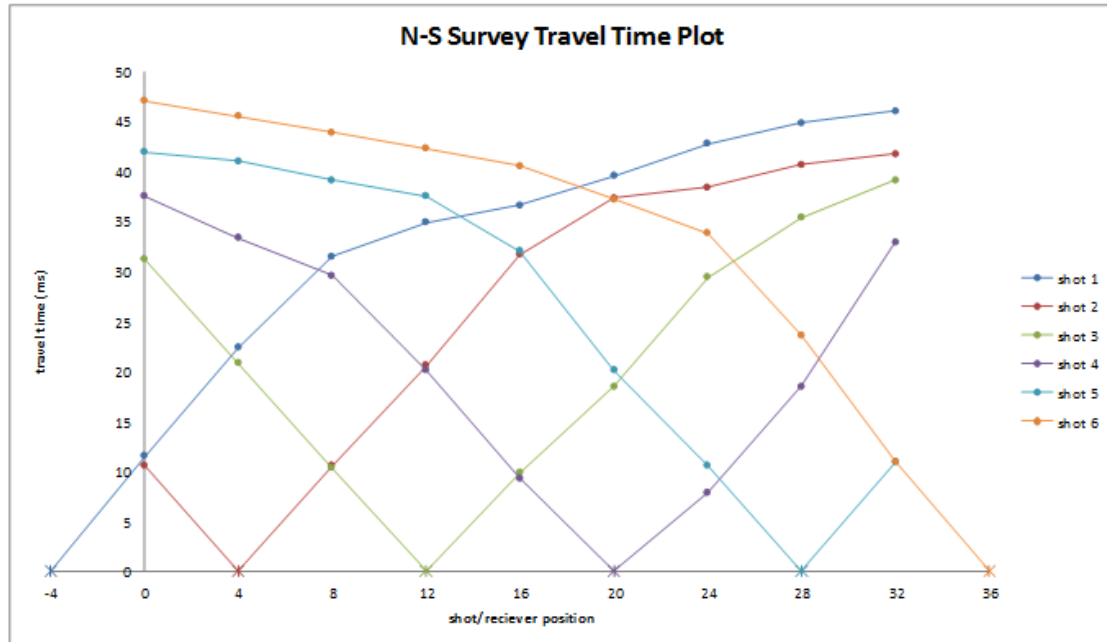


Figure 10: Compiled travel times of the N-S survey which crosses the W-E survey. The stars represent shot locations and the dots represent geophone locations.

Next, time term inversion was performed on the data using the PlotRefa program. This produced 2D models of depth vs. velocity (figures 11 and 12). The W-E survey had a RMS matrix inversion error value of .492783 and the N-S survey had an RMS value of .625203. This is the error from inverting a matrix with mismatched dimensions. Plotrefa recognized any RMS value less than 1.5 to be acceptable.

The quality of the data was checked by testing the reciprocity. Good data should produce the same velocities regardless of direction. Error should fall within 5%. Tables 6 and 7 below list the errors and highlight any that are too high.

Source 1 (m)	Source 2 (m)	Difference (ms)	% error
0	8	-0.35	-2.1
0	16	2.299999	6.7
0	24	-1.599998	-3.9
0	32	0.700001	1.6
0	40	0.150002	0.3
0	48	-0.699997	-1.4
0	56	-0.799992	-1.5
8	16	0.349998	2.2
8	24	-4.099995	-12.2
8	32	-0.549999	-1.4
8	40	-0.5	-1.2
8	48	-1.549999	-3.3
8	56	-0.550003	-1.1
16	24	-1.349998	-8
16	32	3.85	11.4
16	40	-0.649998	-1.6
16	48	-1.746586	-4
16	56	-0.049995	-0.1
24	32	-0.35	-2.2
24	40	1.799999	5.1
24	48	-1.25	-3
24	56	-0.100002	-0.2
32	40	-0.200001	-1.1
32	48	-4.799999	-13.9
32	56	-0.350002	-0.09
40	48	-4.799999	-22.4
40	56	-2.050003	-5.8
48	56	-6.050001	-30.7

Table 6: Reciprocity errors of W-E survey

source 1 (m)	source 2(m)	difference (ms)	%error
4	12	-0.397	-1.8
4	20	-1.507	-4.1
4	28	1.903	4.7
12	20	-0.959	-4.6
12	28	0.562	1.6
20	28	-2.465	-12.1

Table 7: Reciprocity errors for N-S survey

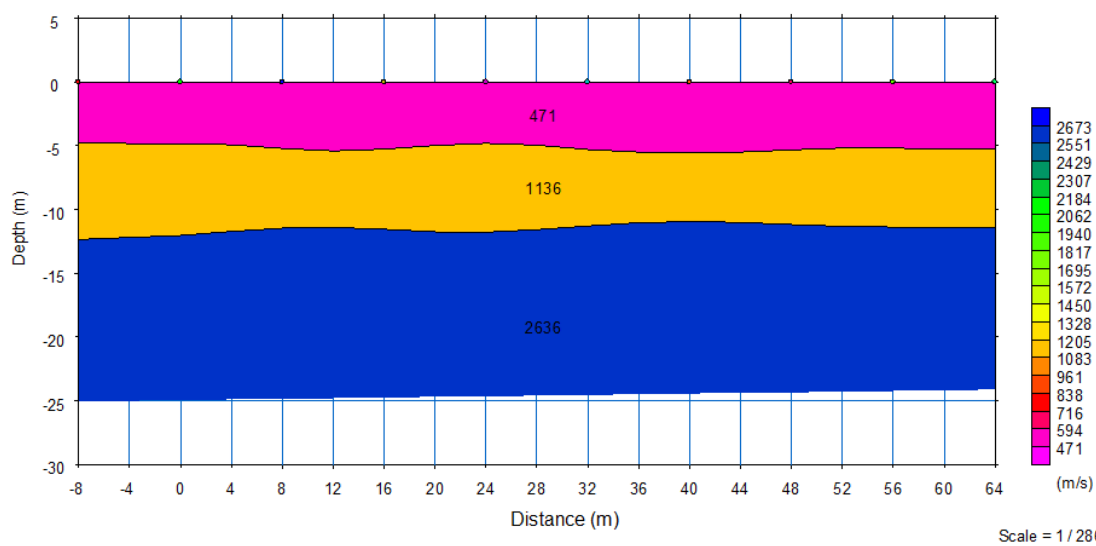


Figure 11: 2D model constructed by time-term inversion of the W-E survey. The layers are defined by color and velocity. The dots along the surface are shot locations.

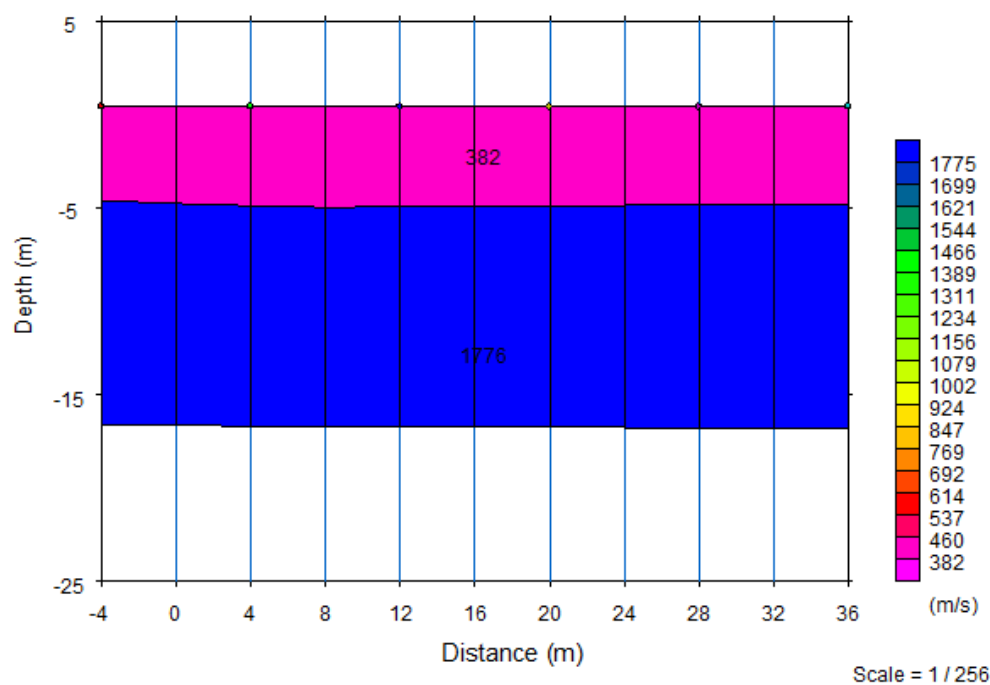


Figure 12: 2D model constructed by time-term inversion of the N-S survey. The layers are defined by color and velocity. The dots along the surface are shot locations.

The time-term models (figures 11 and 12) indicate a slow velocity top layer that is about 5 meters thick. The velocity indicates that the top layer consists of top soil and sand and gravel. The second layer is about 7 meters thick. The velocity indicates a water saturated level or the water table. The third layer has a faster velocity of 2636 m/s. Based on the local geology and the velocity, this layer is composed of fractured limestone which is the Platteville formation. Table 6 below was used to determine the material type based off the velocities.

Material	V_p (m/s)
Air	330
Water	1450–1530
Petroleum	1300–1400
Loess	300–600
Soil	100–500
Snow	350–3000
Solid glacier ice*	3000–4000
Sand (loose)	200–2000
Sand (dry, loose)	200–1000
Sand (water saturated, loose)	1500–2000
Glacial moraine	1500–2700
Sand and gravel (near surface)	400–2300
Sand and gravel (at 2 km depth)	3000–3500
Clay	1000–2500
Estuarine muds/clay	300–1800
Floodplain alluvium	1800–2200
Permafrost (Quaternary sediments)	1500–4900
Sandstone	1400–4500
Limestone (soft)	1700–4200
Limestone (hard)	2800–7000
Dolomites	2500–6500
Anhydrite	3500–5500
Rock salt	4000–5500
Gypsum	2000–3500
Shales	2000–4100
Granites	4600–6200
Basalts	5500–6500
Gabbro	6400–7000
Peridotite	7800–8400
Serpentinite	5500–6500
Gneiss	3500–7600
Marbles	3780–7000
Sulphide ores	3950–6700
Pulverised fuel ash	600–1000
Made ground (rubble etc.)	160–600
Landfill refuse	400–750
Concrete	3000–3500
Disturbed soil	180–335
Clay landfill cap (compacted)	355–380

Table 8: Measured velocities of different materials and rock types (Kohnen 1974)

The calculated velocity of the Platteville limestone is on the low end of the range of possible velocities according to table 6. The presence of many fractures, filled with slower velocity fluids, decreases the velocity of that layer. The study of Mavko (1993) shows the frequency and the amplitude of the signal decreases where fractures are

present. Throughout the data there are low amplitude, low frequency signals around the 40 meter mark (figure 13). This could be a location of a fracture.

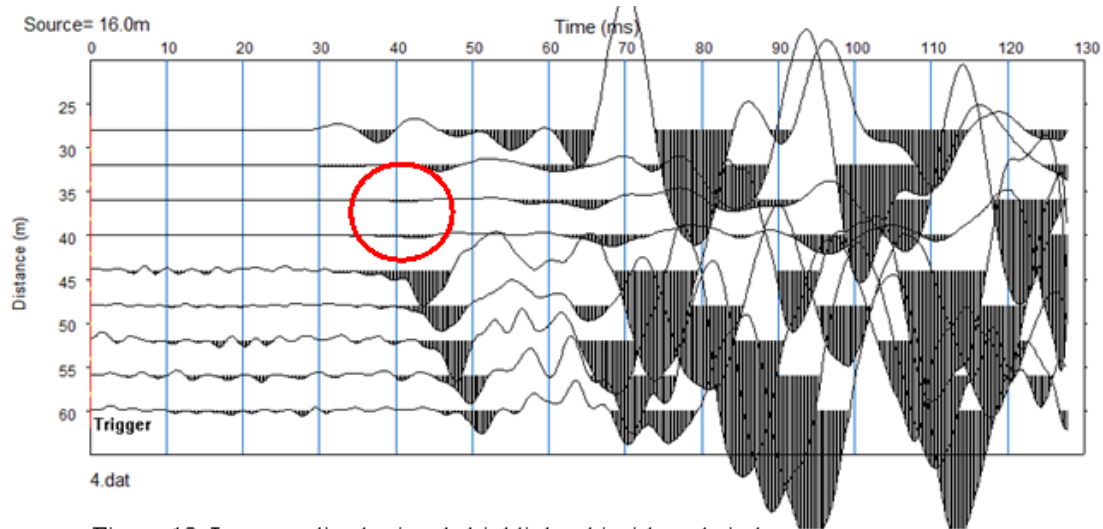


Figure 13: Low amplitude signals highlighted inside red circle.

Conclusions

East River Flats, a city park along the Mississippi River was analyzed using seismic refraction. Calculations and models were done using 1D and 2D time-term inversion methods. The results yielded a 3 layer model. The first layer has a slow velocity of 382-471 m/s which indicated the layer was composed of top soil and sand and gravel. It is about 5 meters thick. The second layer has a velocity of 1136-1776 m/s and is around 7 meters thick. The estimated depth to the water table from the edge of the flats was 5 meters. The calculated depth was also around 5 meters. The estimated and calculated are consistent. The third layer had a velocity of 2636 m/s and was located around 12-13 meters deep. The third layer was identified as the Platteville formation limestone. The slower limestone velocity can be accounted for by the presence of numerous fractures.

There are many future applications for this study. First, it would be useful to collect more data which crosses the original W-E survey line to identify the boundaries of the velocity anomaly. This survey could also be done frequently (monthly, seasonally, etc.) to monitor the rise and fall of the water table. It could also be extended along the Mississippi River either locally or regionally. A larger project would be to map the fractures in the Platteville formation, highlighting areas of high and low fractures. A fracture study would be useful for water well placements and to enhance the understanding of the effects of fractures on seismic velocity.

Bibliography

H.Kohnen. (1974). Temperature Dependence of Seismic Waves in Ice. *Journal of Glaciology*, 144-147.

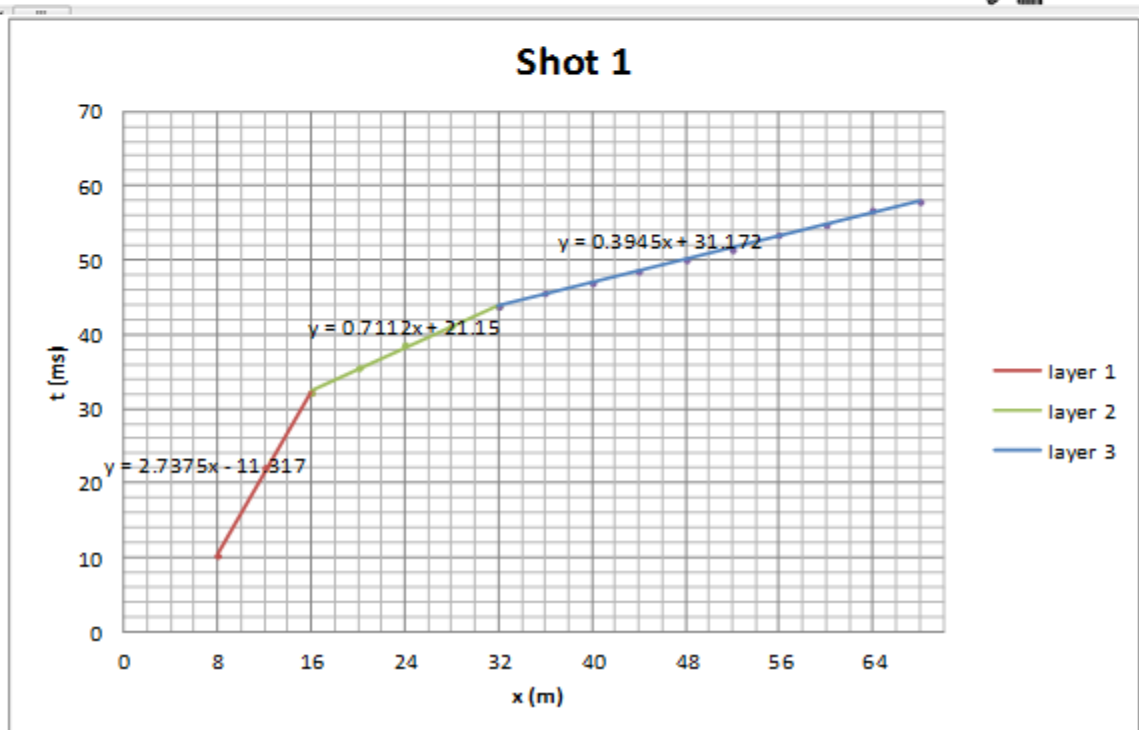
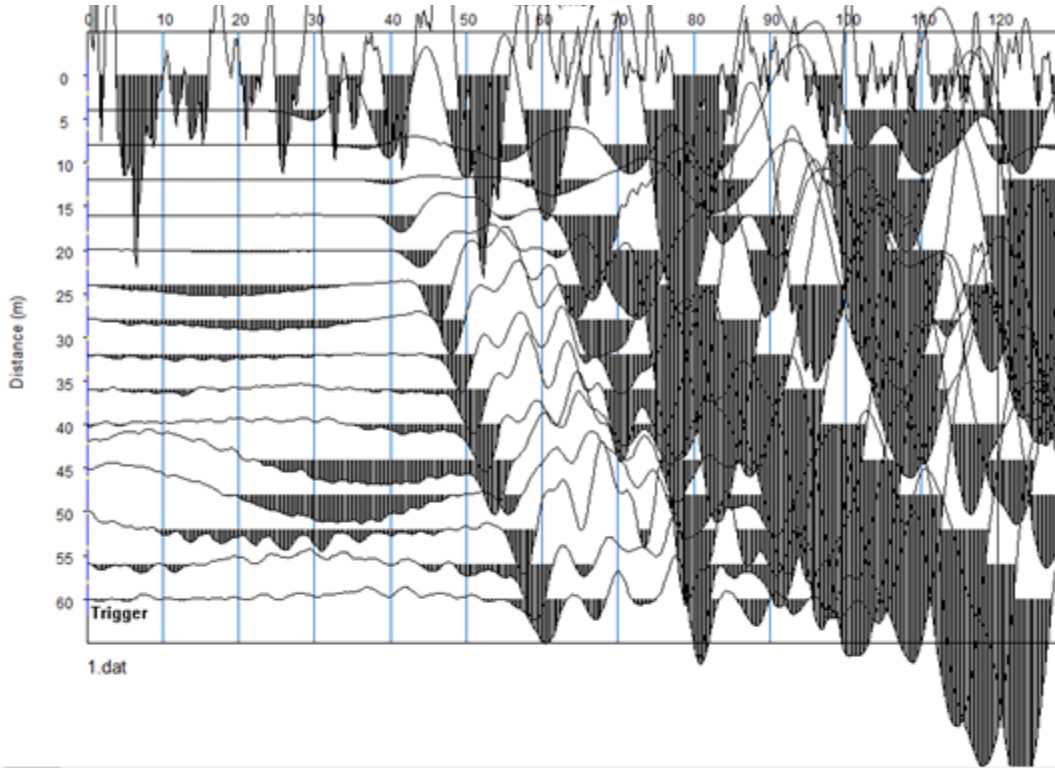
Madigan, T. (2003, august 5). River of History. national park services.

Mavko, G. (1993). Rock Physics Constraints on Seismic Signatures of Fractures.

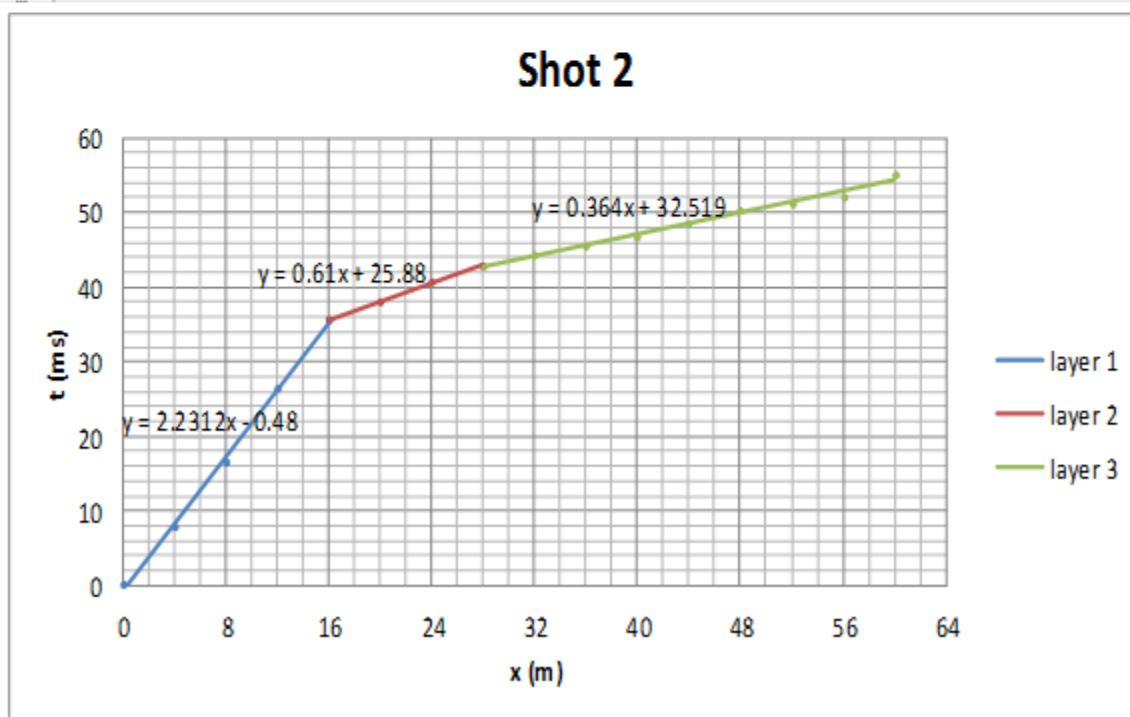
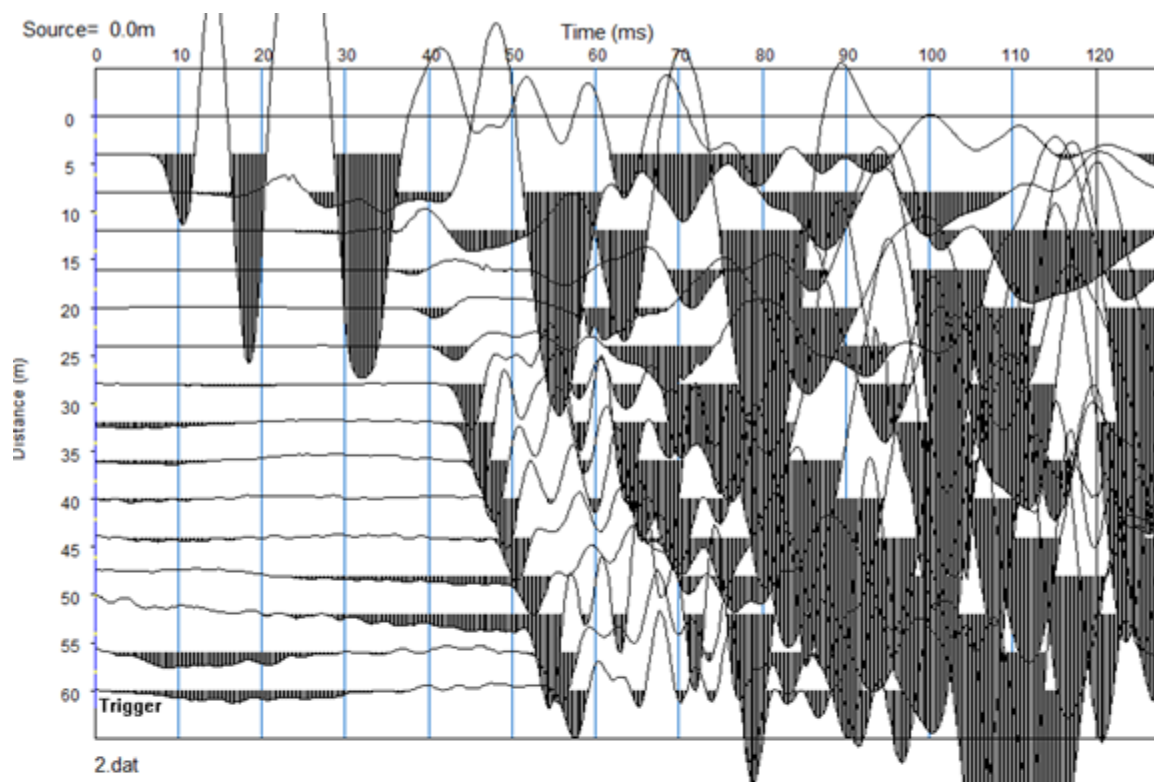
Appendix

W-E Survey Shots

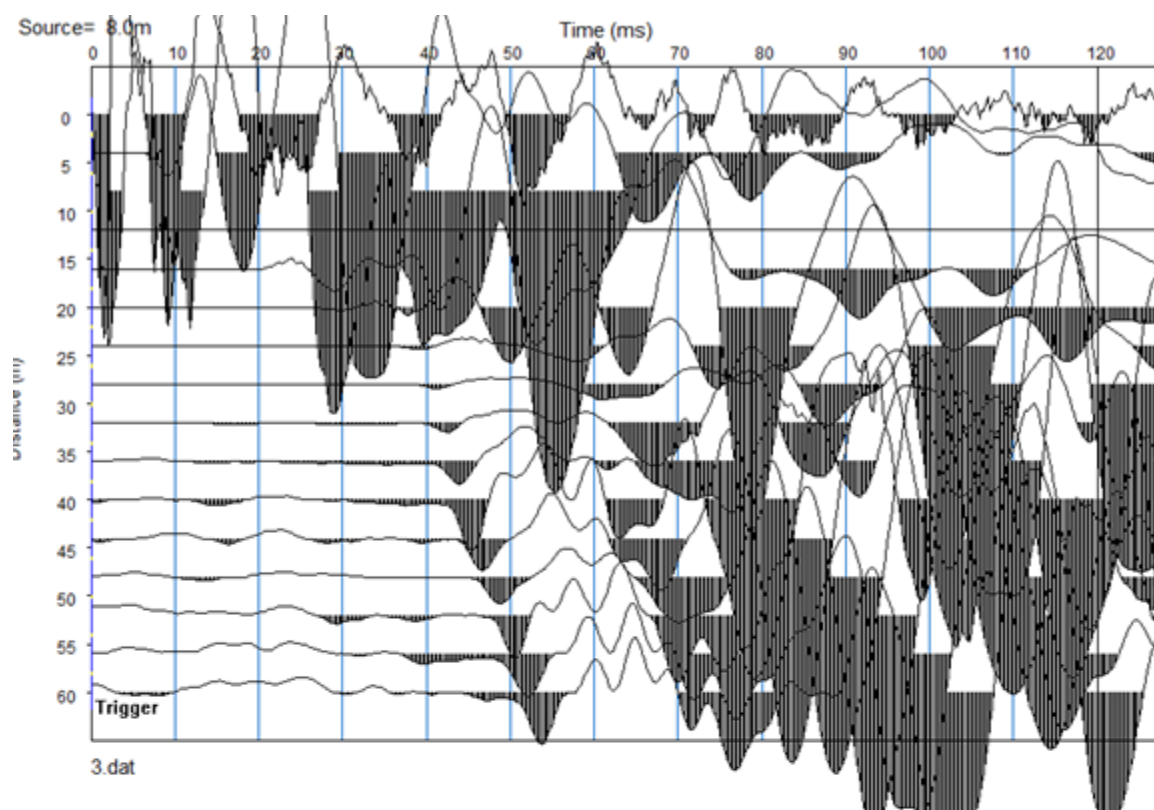
Shot 1 (-8 m)



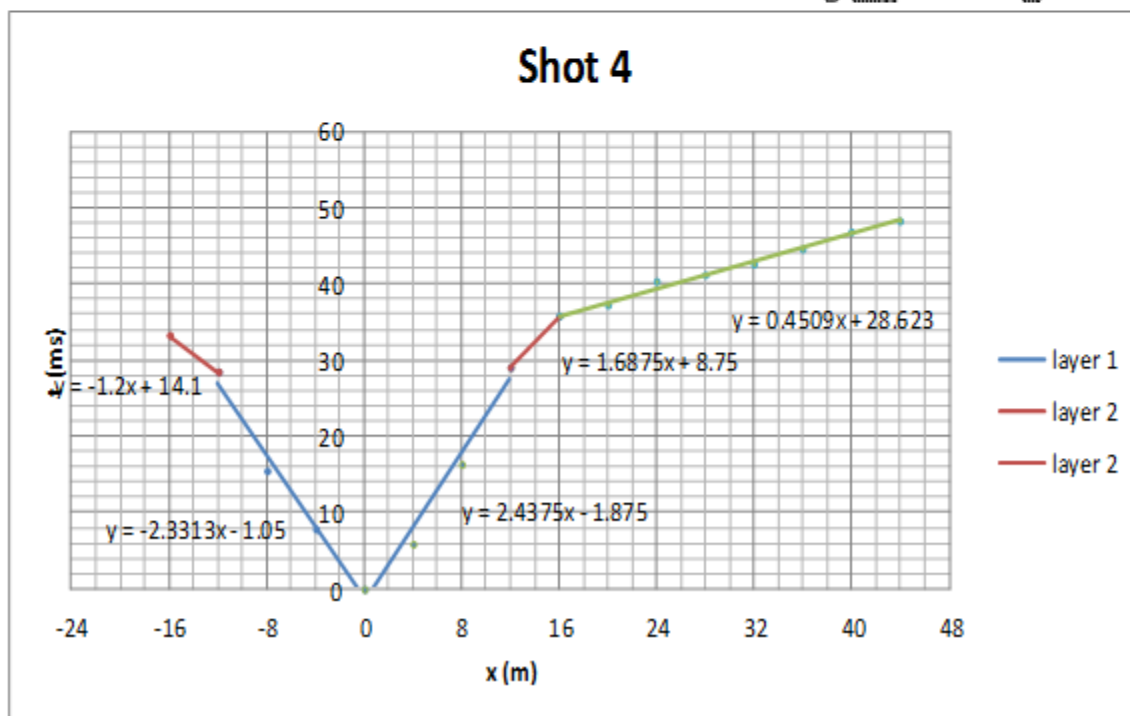
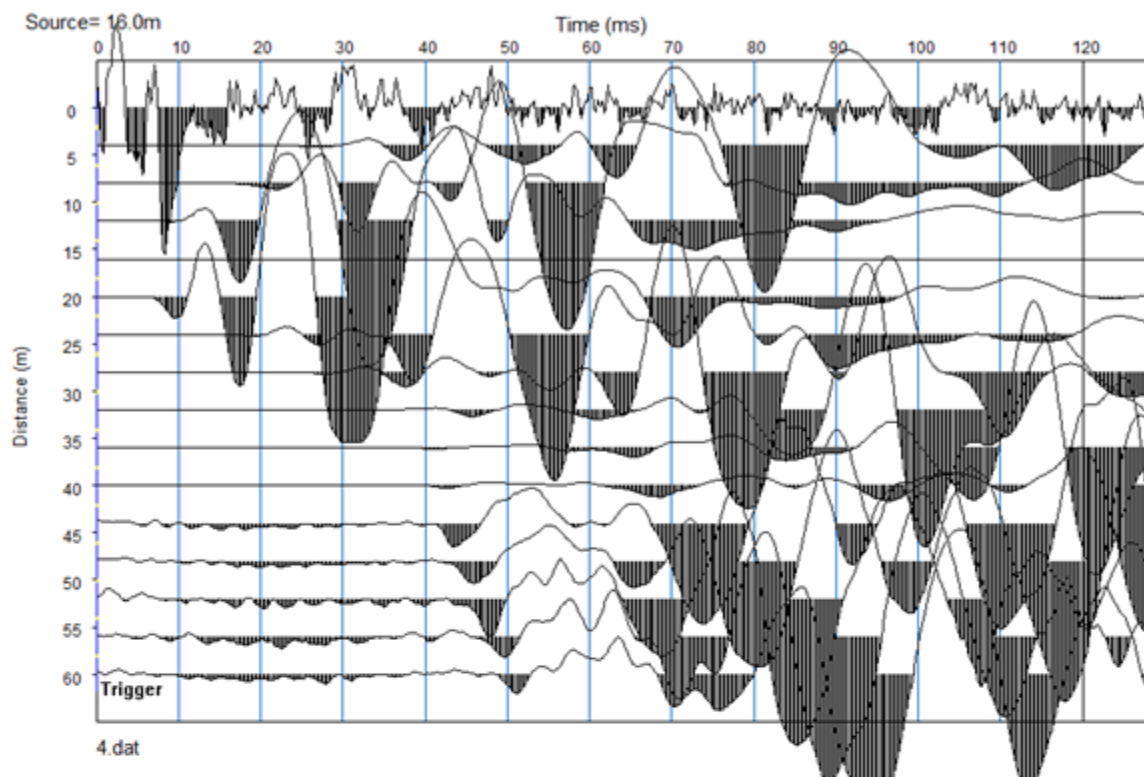
Shot 2 (0m)



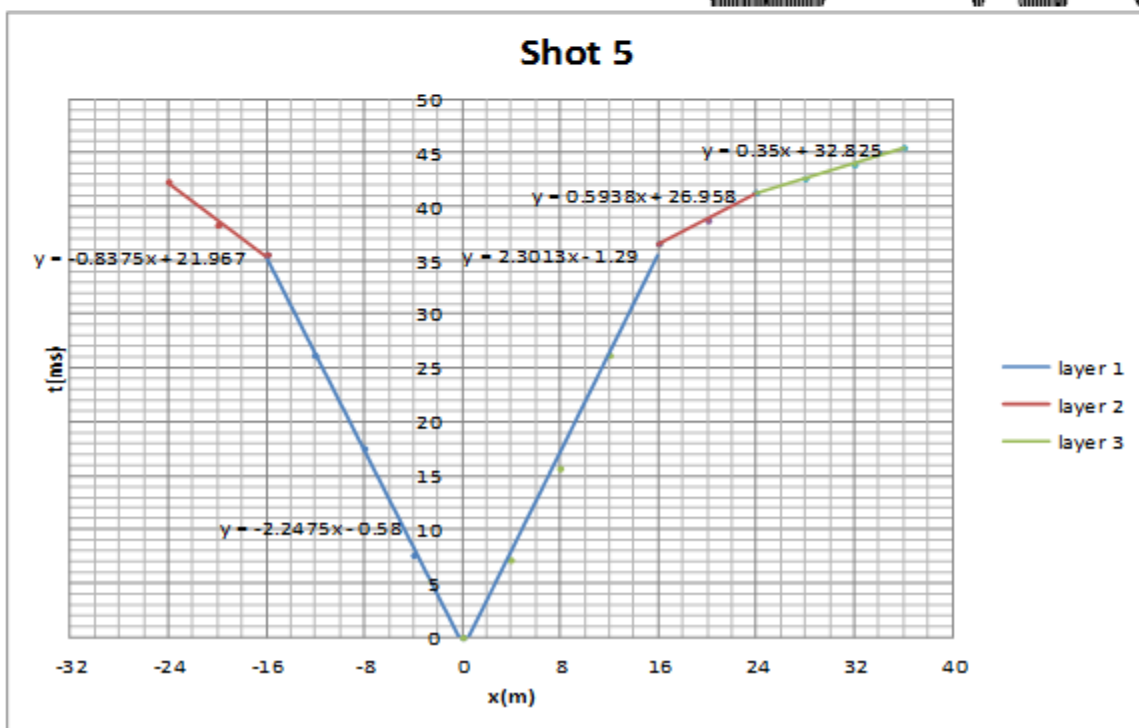
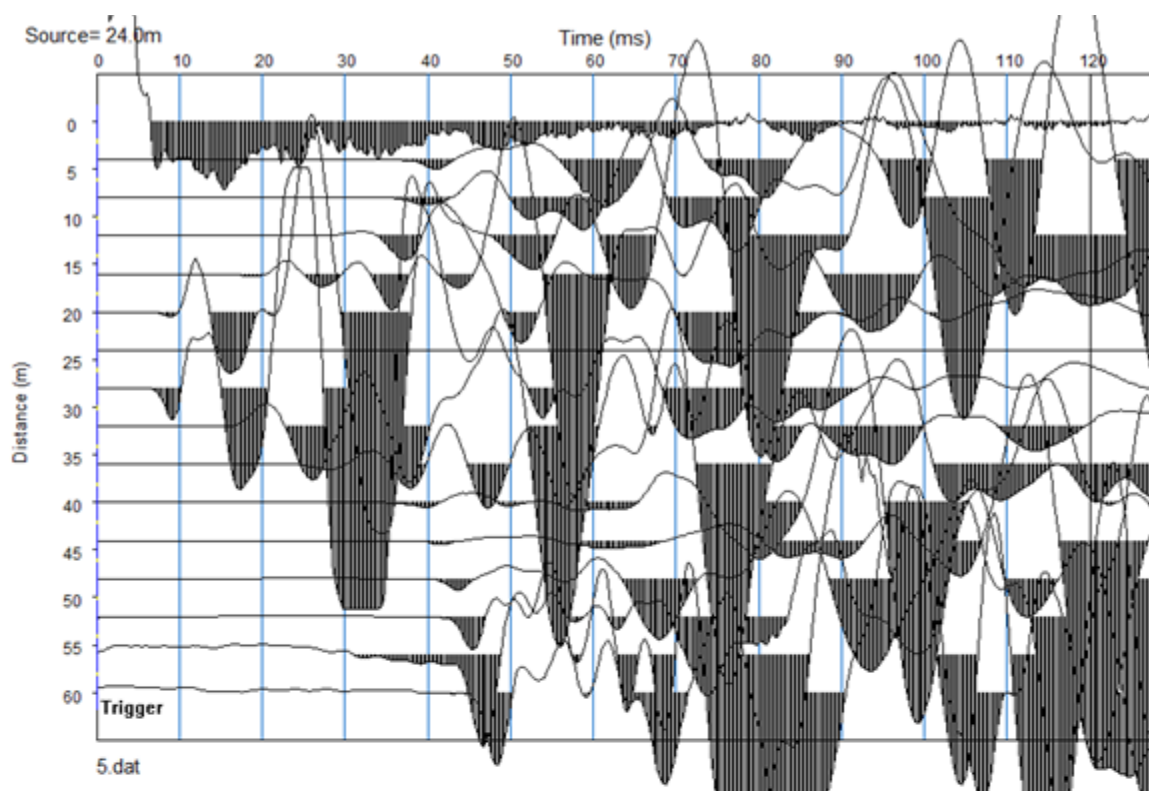
Shot 3 (8m)



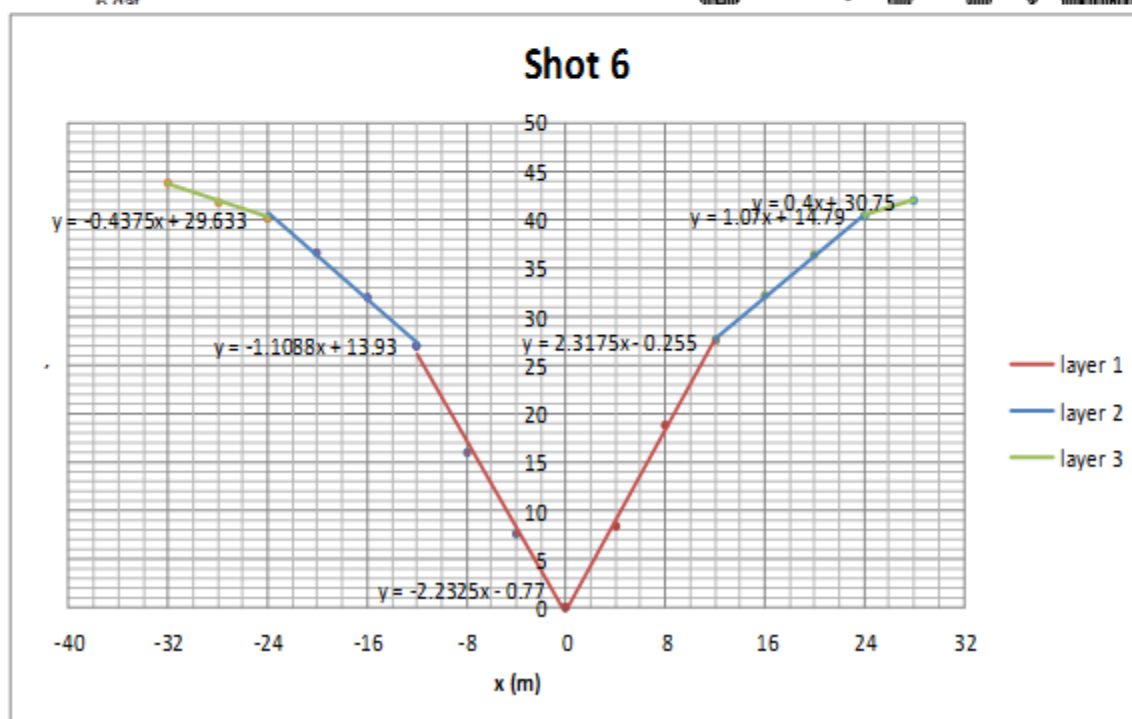
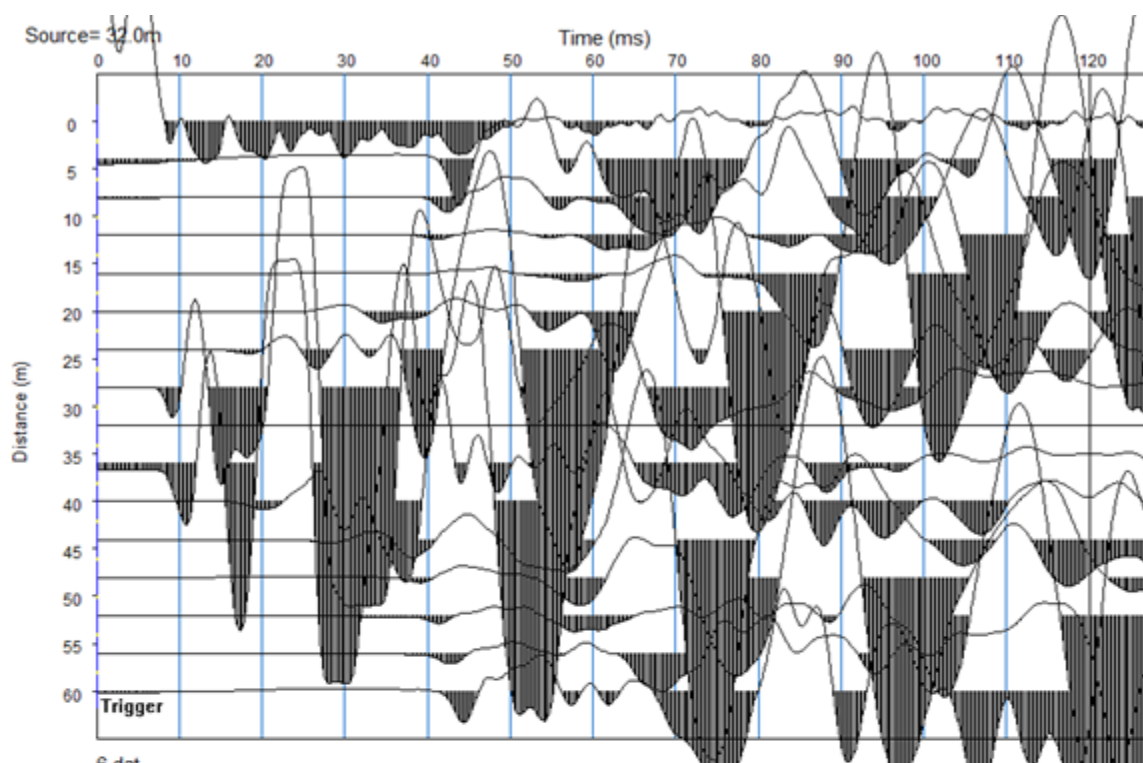
Shot 4 (16m)



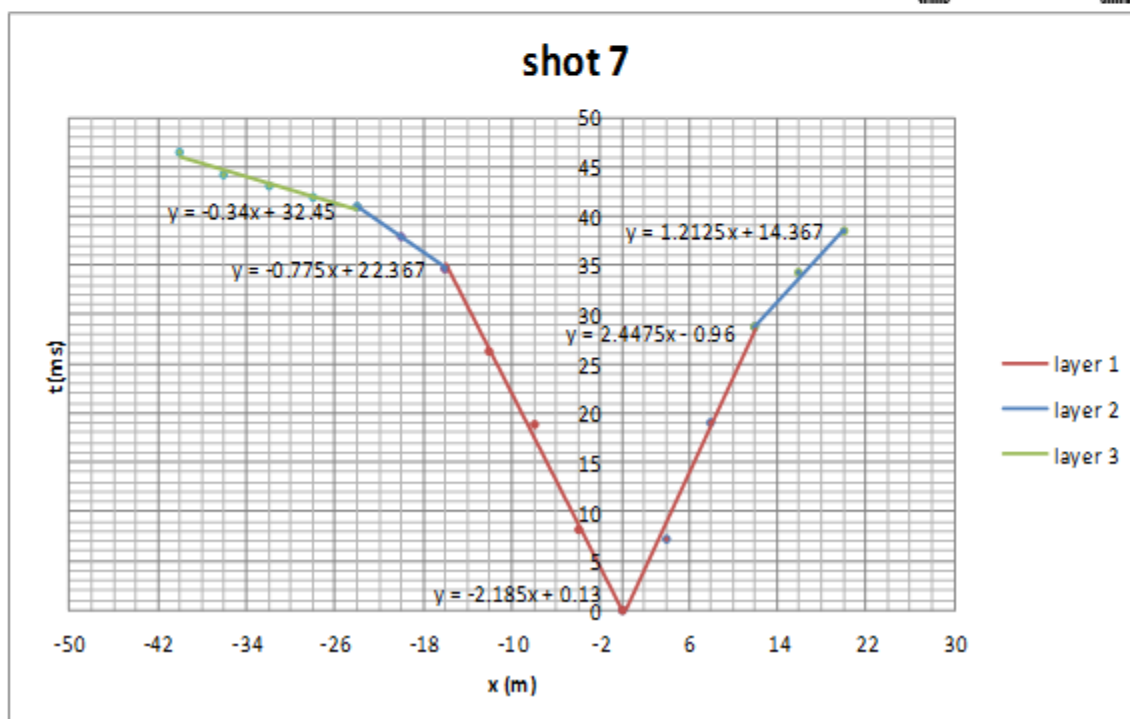
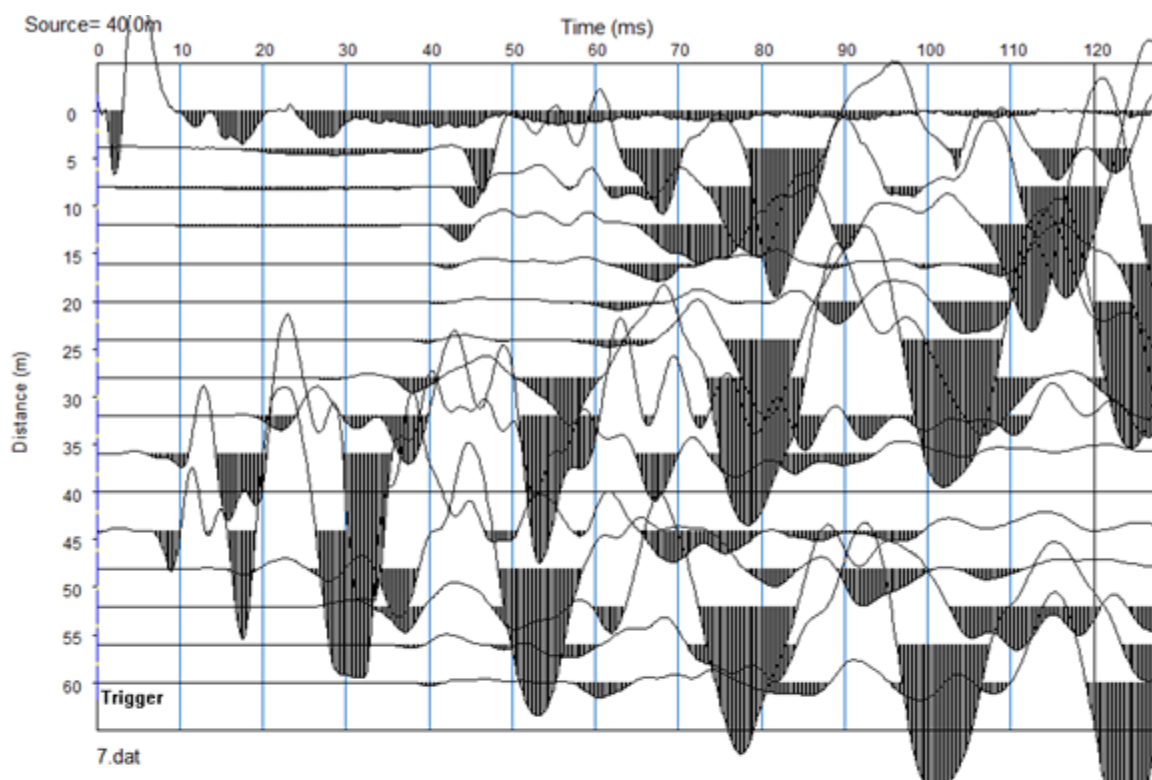
Shot 5 (24m)



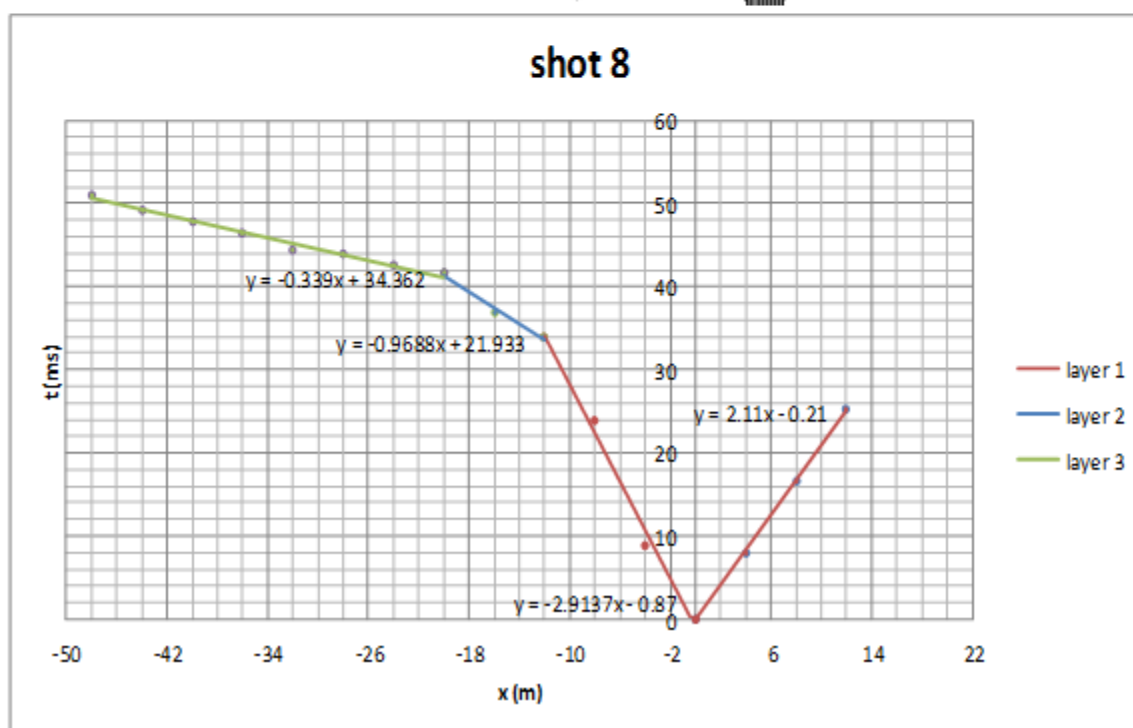
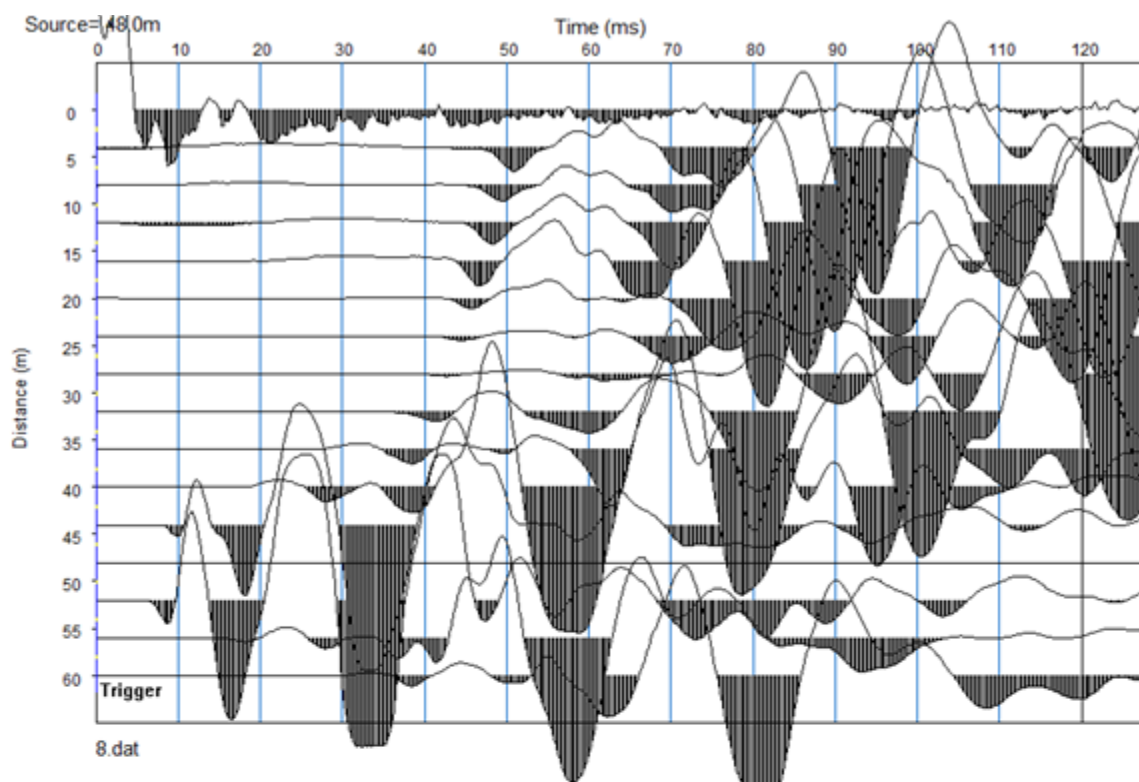
Shot 6 (32m)



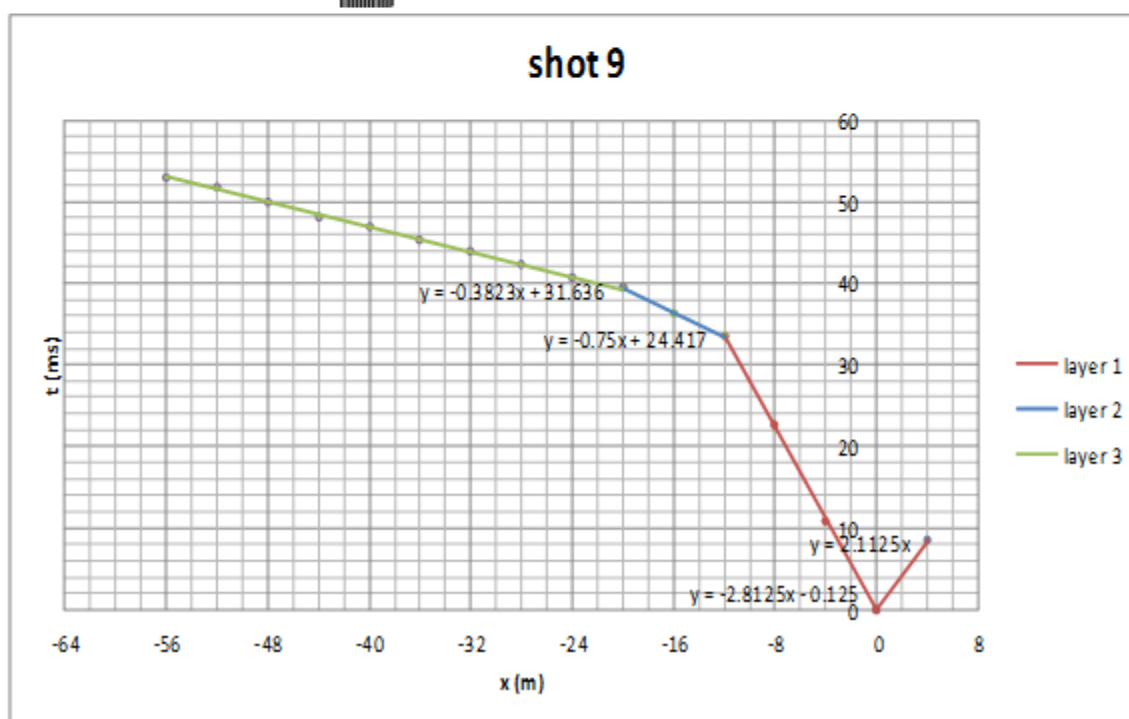
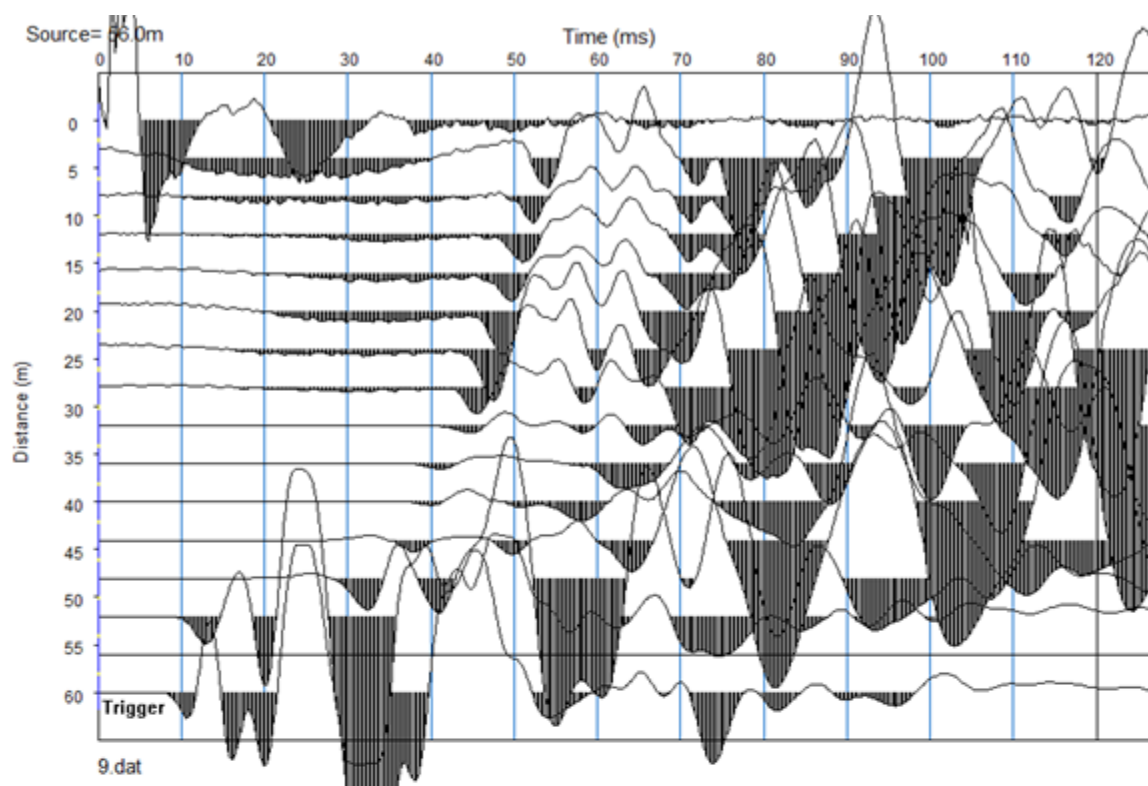
Shot 7 (40m)



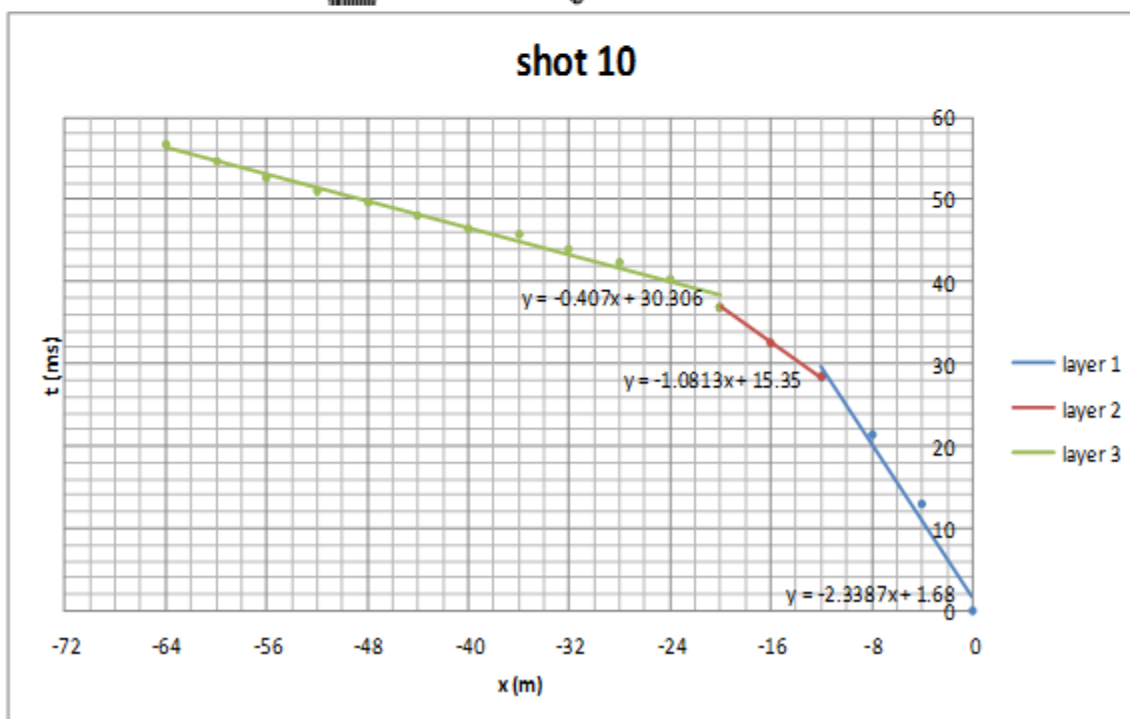
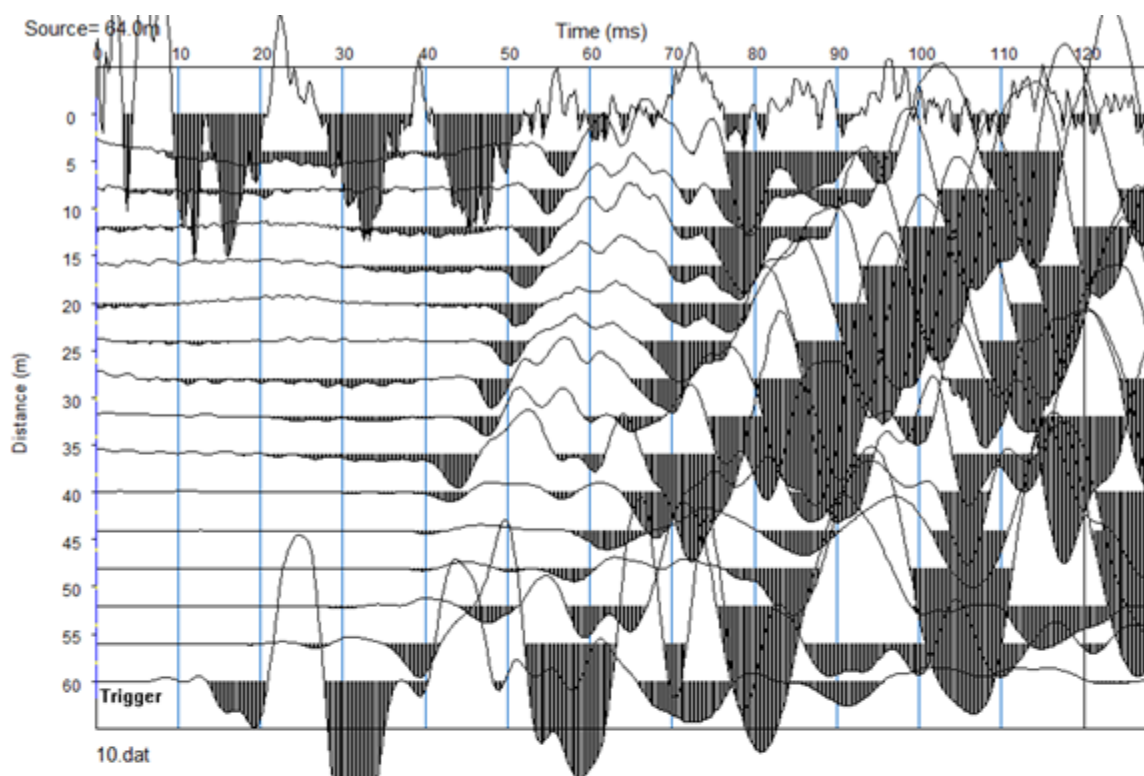
Shot 8 (48m)



Shot 9 (56m)

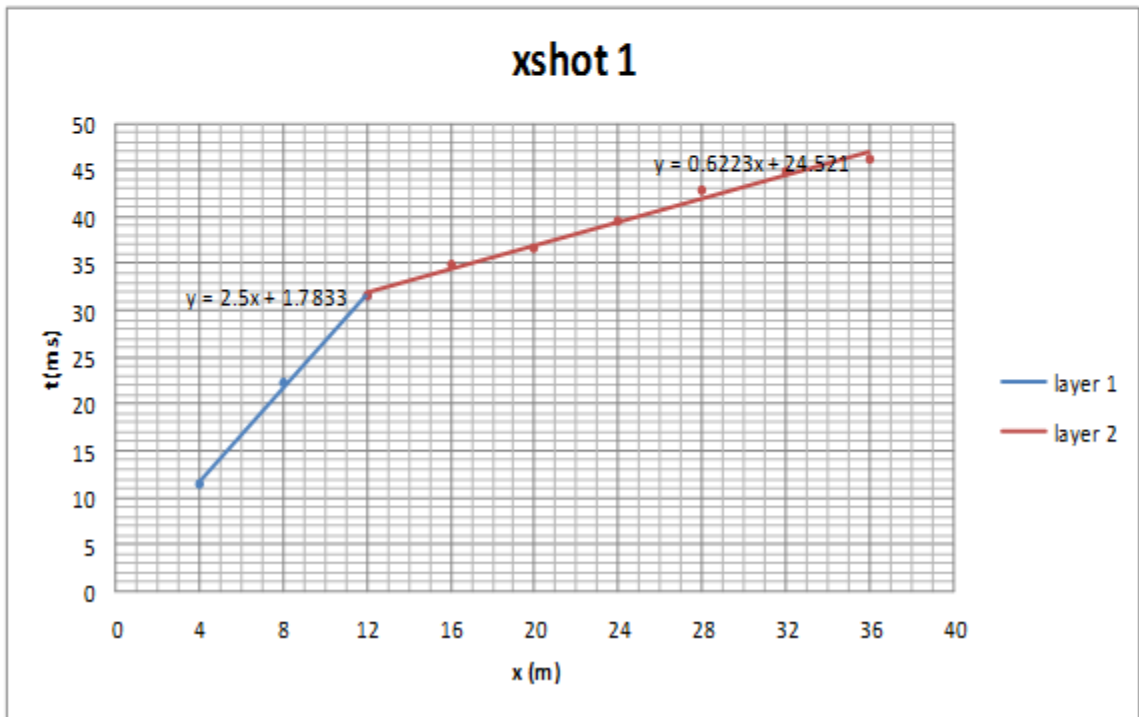
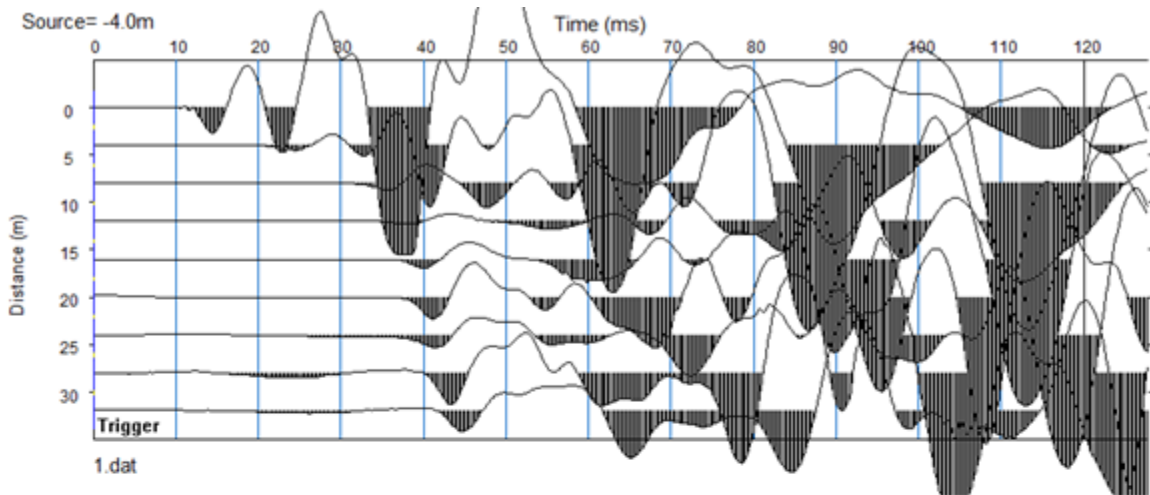


Shot 10 (64m)

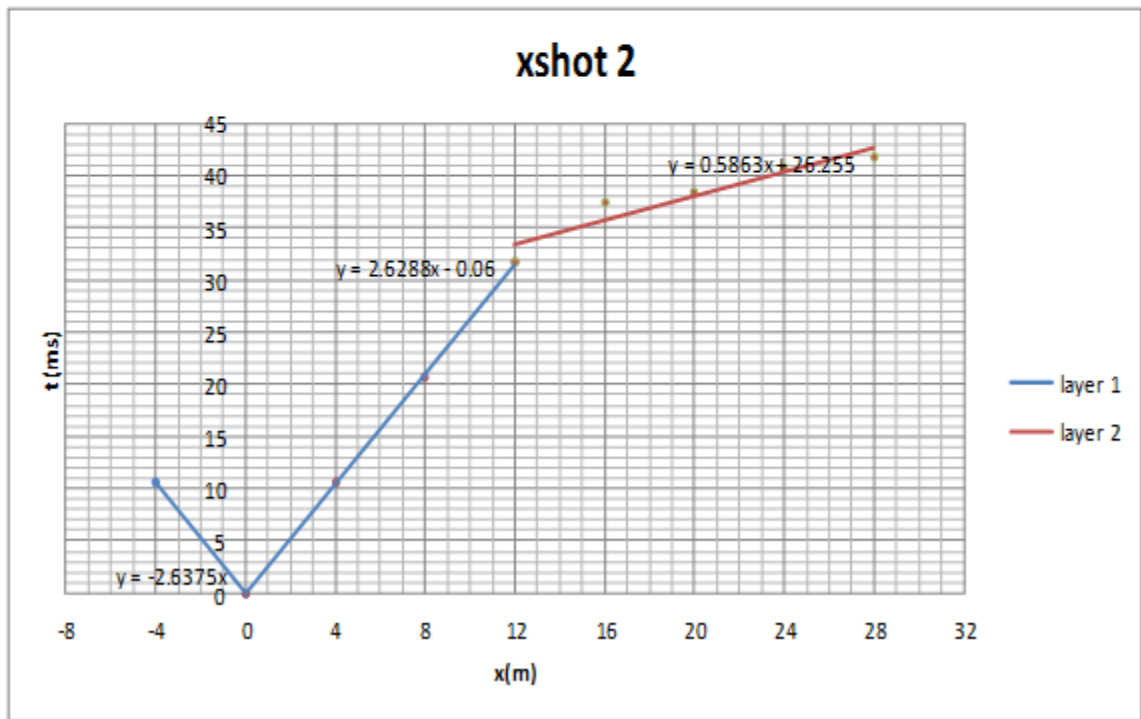
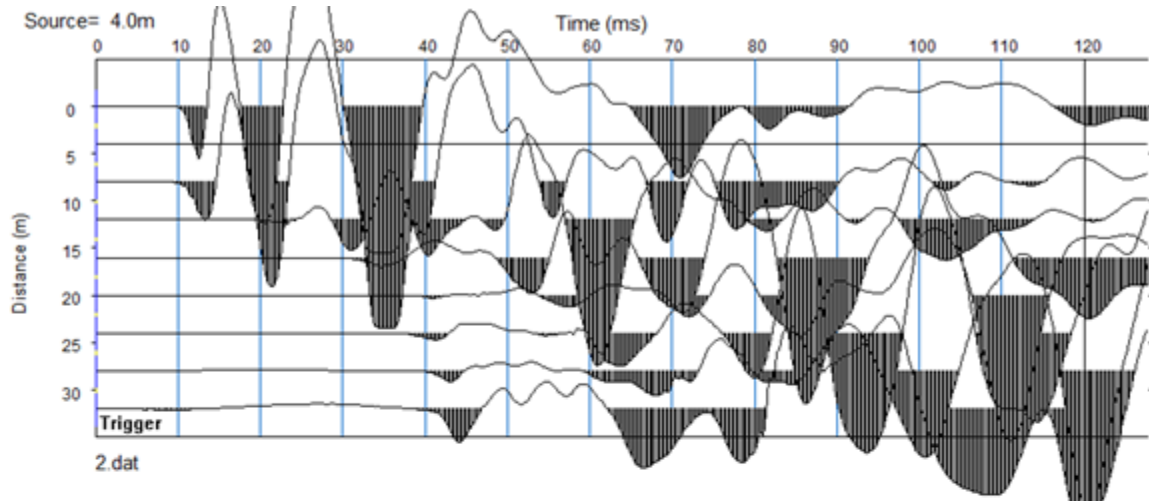


N-S Survey

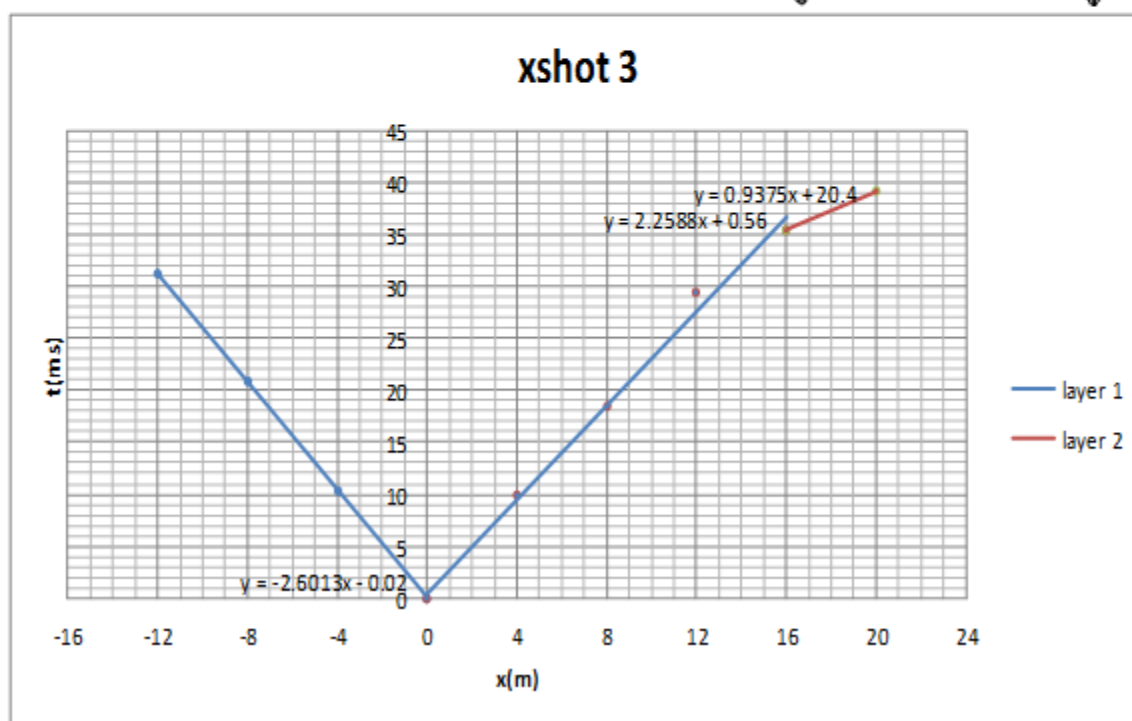
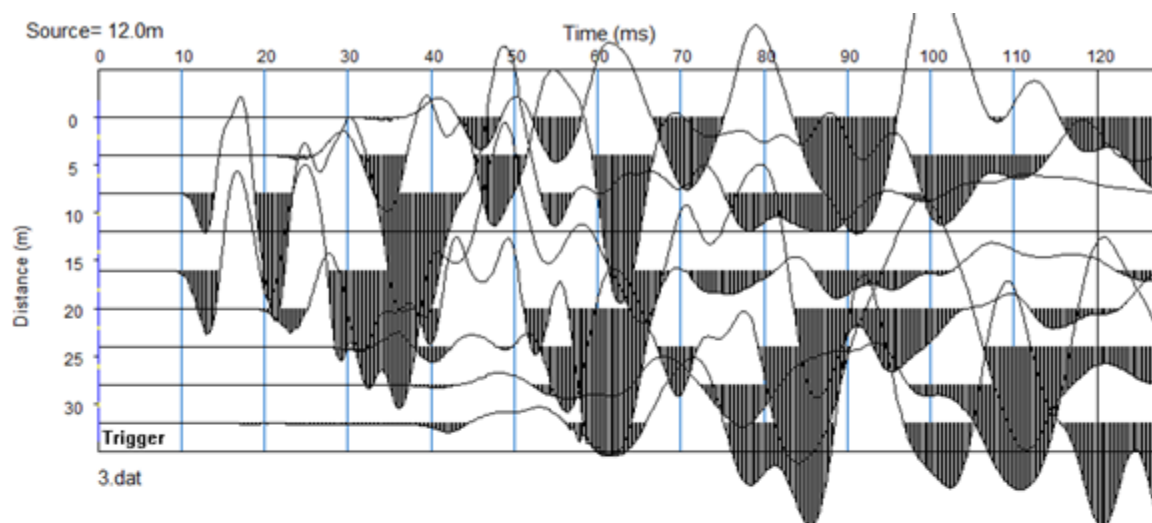
Shot 1 (-4m)



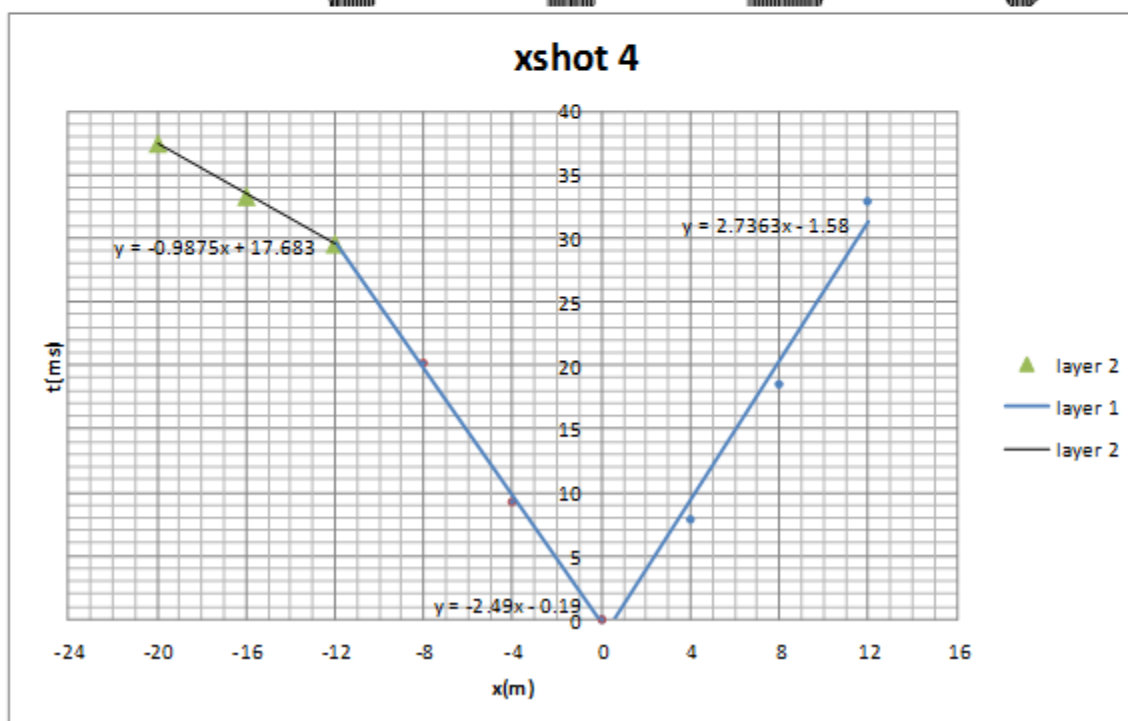
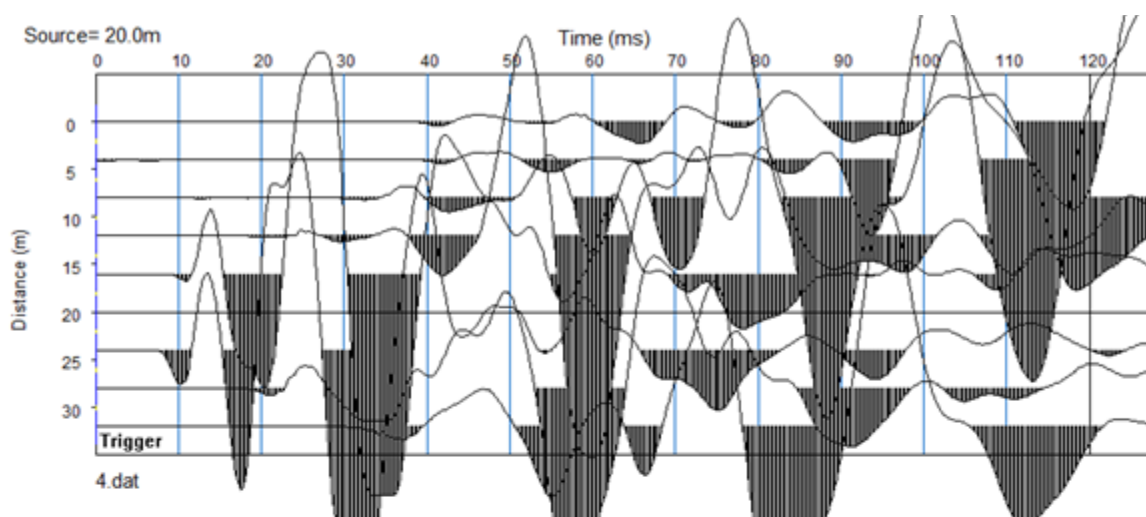
Shot 2 (4m)



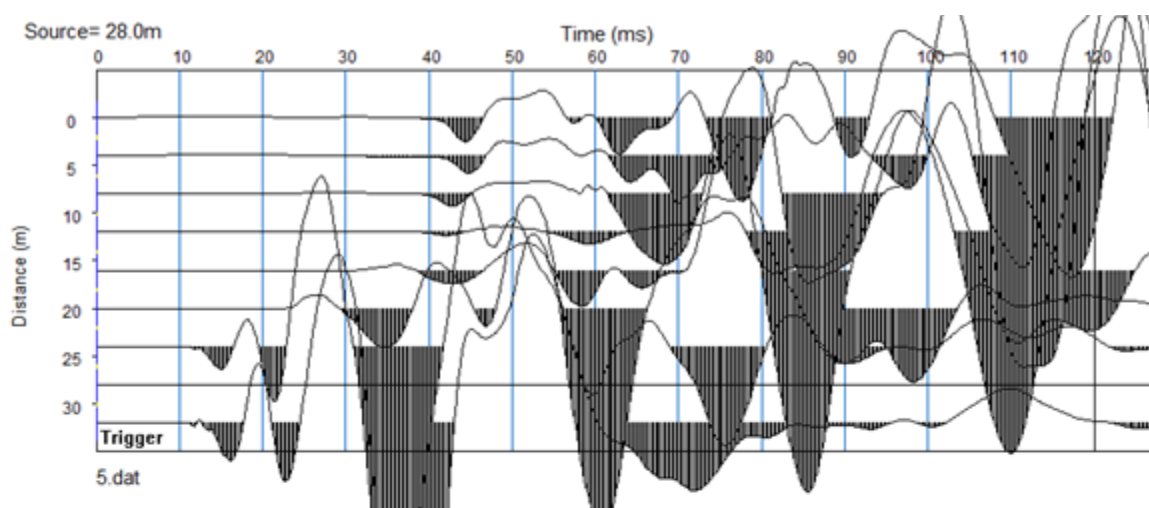
Shot 3 (12m)



Shot 4 (20m)



Shot 5 (28m)



Shot 6 (36m)

